Supporting information

Elucidating the Ordering in Self-Assembled Glycocalyx Mimicking Supramolecular Copolymers in Water

*Simone I. S. Hendrikse,#† Lu Su,#† Tim P. Hogervorst,‡ René P. M. Lafleur,† Xianwen Lou,† Gijsbert A. van der Marel,‡ Jeroen D. C. Codee,‡ and E. W. Meijer†**

† Institute for Complex Molecular Systems, Eindhoven University of Technology, P.O. Box 513, 5600 MB Eindhoven, The Netherlands. ‡ Department of Bio-organic synthesis, Leiden Institute of Chemistry, Leiden University, Leiden, The Netherlands.

* e.w.meijer@tue.nl

Table of Contents

1. Materials and instrumentations

Unless stated otherwise, all reagents and chemicals were obtained from commercial sources at the highest purity available and used without further purification. All solvents were of AR quality and purchased from Biosolve. Water was purified on an EMD Milipore Mili-Q Integral Water Purification System. Reactions were followed by thin-layer chromatography (precoated 0.25 mm, 60-F254 silica gel plates from Merck), and flash chromatography was run with silica gel (40–63 μm, 60 Å from Screening Devices b.v.). Dry solvents were obtained with an MBRAUN Solvent Purification System (MB-SPS). Automated column chromatography was performed using Biotage® SNAP-KP SIL cartridges.

Compounds 2,3,4,6-tetra-*O*-benzoyl-α-D-mannopyranosyl trichloroacetimidate[1] and BTA-OEG_4[2] were synthesized according to literature procedures.

NMR spectra were recorded on Bruker 400 MHz Ultrashield spectrometers (400 MHz for ^{1}H NMR). Deuterated solvents used are indicated in each case. Chemical shifts (δ) are expressed in ppm and are referred to the residual peak of the solvent. Peak multiplicity is abbreviated as s: singlet; d: doublet; t: triplet; dt: doublet of triplets; ddt: doublet of doublets of triplets; td: triplet of doublets; tt: triplet of triplets; q: quartet; qd: quartet of doublets; m: multiplet.

Matrix assisted laser absorption/ionization-time of flight (MALDI-TOF) mass spectra were obtained on a PerSeptive Biosystems Voyager DE-PRO spectrometer using α-cyano-4-hydroxycinnamic acid (CHCA) or *trans*-2-[3-(4-*tert*-butylphenyl)-2-methyl-2-propenylidene]-malononitrile (DCTB) as matrix.

Fourier transform infrared (FT-IR) spectroscopy measurements were performed on a Perkin Elmer FT-IR Spectrum Two apparatus.

Ultraviolet-visible (UV-vis) absorbance spectra were recorded on and a Jasco V-650 UV-vis spectrometer or a Jasco V-750 UV-vis spectrometer with a Jasco ETCT-762 temperature controller.

Circular dichroism (CD) measurements were carried out on JASCO J-815 spectrometer at room temperature with the following settings: Sensitivity = 1000 mdeg (low), scan rate = 100 nm/min, bandwidth = 1 nm, response time = 0.5 s and number of accumulations = 3. Variable-temperature measurements were performed using a CDF-426S/15 Peltier type temperature controller in the temperature range of 293-363 K.

Cryogenic transmission electron microscopy (cryo-TEM) was performed on samples with a concentration of 250 or 500 μM. Vitrified films were prepared in a 'Vitrobot' instrument (FEI Vitrobot™ Mark III, FEI Company) at 22 °C and at a relative humidity of 100%. In the preparation chamber of the 'Vitrobot' a 3 μL sample was applied on a Lacey film (LC200-CU, Electron Microscopy Sciences). These films were surface plasma treated just prior to use (Cressington 208 carbon coater operating at 5 mA for 40 s). Excess sample was removed by blotting using filter paper for 3 seconds at –3 mm, and the thin film thus formed was shot (acceleration about 3 g) into liquid ethane just above its freezing point. Vitrified films were transferred into the vacuum of a CryoTITAN equipped with a field emission gun that was operated at 300 kV, a post-column Gatan energy filter, and a 2048 x 2048 Gatan CCD camera. TEM under dry conditions was performed with samples at a concentration of 50 μM. 2 μL droplets were cast on surface plasma treated copper grids featuring a carbon film (CF300-Cu,

Electron Microscopy Sciences), and excess solvent was removed manually with filter paper. The dried grids were transferred into the vacuum of a Tecnai Sphera microscope. This microscope is equipped with a LaB_6 filament that was operated at 200 kV, and a bottom mounted Ceta 4096x4096 CMOS camera. Microscopy images were taken at low dose conditions for the vitrified samples, starting at a magnification of 6500 with a defocus setting of 40 µm. Subsequently images were acquired at 24000 magnification and at a defocus of 10 µm or 15 µm. High magnification TEM images were acquired at a magnification of 24000 and at a defocus of 10 µm using normal dose conditions. Images were post-processed by enhancing the contrast and brightness.

Dynamic light scattering measurements were recorded on an ALV/CGS-3 MD-4 compact goniometer system equipped with a multiple tau digital real time correlator (ALV-7004) and a solid state laser (λ = 532 nm; 40 mW).

Micro-differential scanning calorimetry (Micro-DSC) was performed on a TA Instruments Multicell DSC. About 1.0 mL of material was prepared in Hastelloy ampoules and characterized using the following heating program: Equilibrate at 25 °C, 25 °C to 90 °C at 60 °C h^{-1}, equilibrate for 15 min, 90 °C to 5 °C at 60 °C h^{-1}, equilibrate for 15 min, 5 °C to 90 °C at 60 °C h^{-1}, equilibrate for 15 min, 90 °C to 5 °C at 60 °C h^{-1}, equilibrate for 15 min, 5 °C to 90 °C at 60 °C h^{-1}, equilibrate for 15 min, 90 °C to 25 °C at 60 °C h^{-1}. Baseline curves of MQ water were subtracted from sample curves.

Hydrogen/deuterium exchange mass spectrometry (HDX-MS) measurements were carried out using a XevoTM G2 QTof mass spectrometer (Waters) with a capillary voltage of 2.7 kV and a cone voltage of 20 V. The source temperature was set at 100°C, the desolvation temperature at 400°C, and the gas flow at 500 L/h. The sample solutions subjected to HDX were introduced into the mass spectrometer using a Harvard syringe pump (11 Plus, Harvard Apparatus) at a flow rate of 50 µL/min.

Small angle X-ray scattering measurements were performed on a SAXSLAB GANESHA 300 XL SAXS system equipped with a GeniX 3D Cu Ultra Low Divergence micro focus sealed tube source producing X-rays with a wavelength λ = 1.54 Å at a flux of 1x108 ph s-1 and a Pilatus 300K silicon pixel detector with 487 x 619 pixels of 172 µm2 in size placed at a sample-to-detector distance of 713 mm respectively to access a q-range of $0.15 \leq q \leq 4.47$ nm-1 with $q = 4\pi/\lambda(\sin\theta/2)$. Silver behenate was used for calibration of the beam centre and the q range. Samples were contained in 2 mm quartz capillaries (Hilgenberg Gmbh, Germany). The two-dimensional SAXS patterns were brought to an absolute intensity scale using the calibrated detector response function, known sample-to-detector distance, measured incident and transmitted beam intensities, and azimuthally averaged to obtain one dimensional SAXS profiles. The scattering curves of the supramolecular polymers were obtained by subtraction of the scattering contribution of the solvent and quartz cell. Finally, the absolute calibration of the scattering curves was verified using the known scattering cross-section per unit sample volume, $d\Sigma/d\Omega$, of water, which is 0.01632 cm^{-1} at T = 20 °C.

2. Synthetic procedures

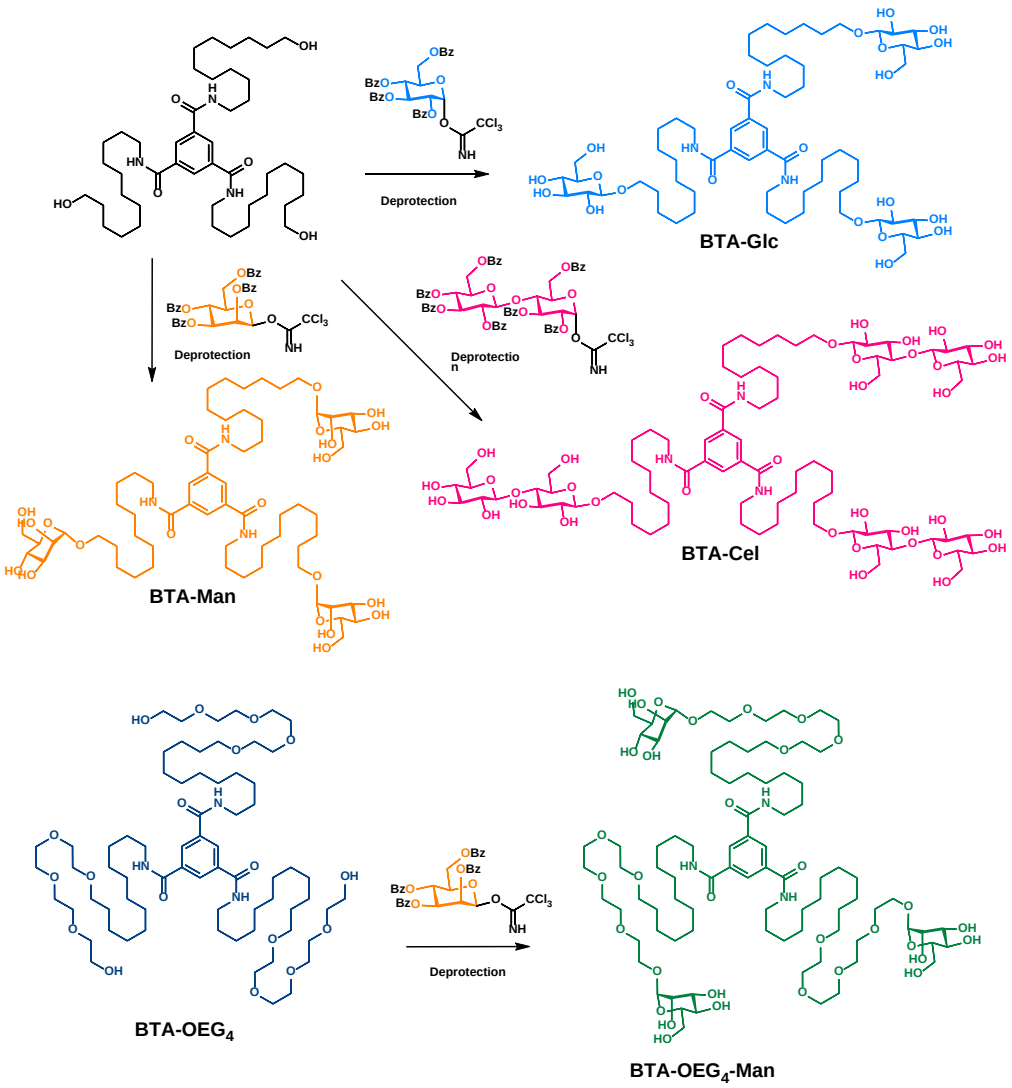

Scheme S1: Synthesis pathway to the BTA-saccharide variants.

Synthesis of BTA-C12-OH **(BTA-OH)**. 12-Amino-1-dodecanol (3.3 eq) was dissolved in chloroform and triethylamine (Et_3N)was added (3.3 eq), after which the solution was cooled on ice under an argon atmosphere. To the solution 1,3,5-benzenetricarbonyltrichloride (1 eq) dissolved in chloroform was dropwise added over 30 minutes on ice. After 15 minutes the ice was removed and the reaction was allowed to stir overnight at room temperature. The crude was purified on silica using a gradient of 5-15% methanol in chloroform yielding compound **X1** in a 55-66% yield with minor impurities of the 2-arm functionalized BTA. ^{1}H NMR (400 MHz, MeOD) δ ppm, 8.36 (s, 3H), 3.53 (t, 6H), 3.39 (t, 6H), 1.63 (m, 6H), 1.51 (m, 6H), 1.31 (m, 48H). ^{13}C NMR (101 MHz, CD_3OD) δ ppm, δ 167.25 (C=O), 135.47 (CH_{arom}), 128.32 (CH_{arom}), 61.61 (C-OH), 39.83 (C-NH), 32.27, 29.36-29.07, 26.70, 25.56. LCMS; Mw_{calc} = 760.16 g/mol m/z_{obs} = 760.58 $[M+H]^+$.

Synthesis of BTA-Glc

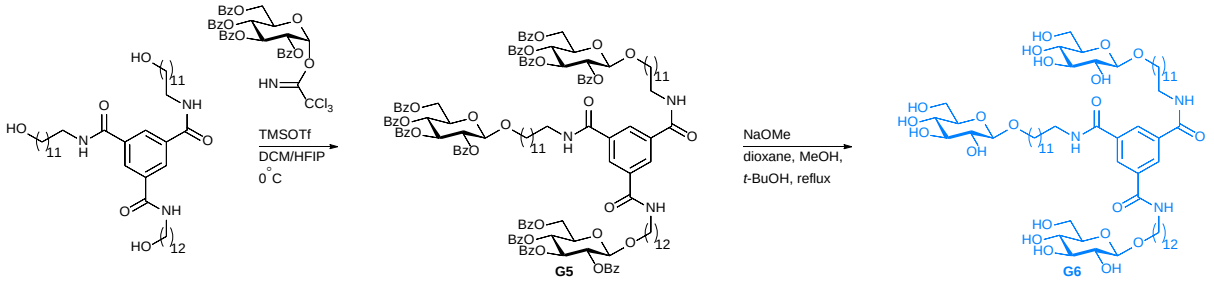

Scheme S2: Synthetic approach to **BTA-Glc**.

***N*^{1}, *N*^{3}, *N*^{5}-Tris(2,3,4,6-tetra-*O*-benzoyl-1-*O*-dodecyl-*β*-D-glucopyranoside)-benzene-1,3,5-tricarboxamide (G5).** Acceptor **BTA-OH** (0.72 g, 0.95 mmol, 1 eq) and 2,3,4,6-tetra-*O*-benzoyl-α-D-glucopyranosyl trichloroacetimidate[3] (2.18 g, 2.94 mmol, 3.1 eq) were combined and co-evaporated 3x with toluene under N_2 atmosphere. The reaction mixture was dissolved in DCM/HFIP (41 mL, 0.023 M, 4/1, v/v) and flame dried molecular sieves (3Å) were added and the mixture was stirred at r.t. for 30 min, after which it was cooled to 0 ˚C. Trifluoromethanesulfonic acid (TfOH, 34 µL, 0.38 mmol, 0.4 eq) was added dropwise and the mixture was stirred at 0 ˚C for 2.5 hour after which it was quenched with Et_3N (0.3 mL) diluted in DCM and washed with NaOH (1 M, aq., 1x), HCl (1 M, aq., 1x) and $NaHCO_3$ (sat aq. 1x). The organic layer was dried over $MgSO_4$, filtered and concentrated. After purification by silica gel column chromatography (1/1 Et_2O/PE, v/v -> 100% Et2O -> 2/8 EtOAc/Et_2O, v/v) a mixture of title compound **G5** and a minor impurity (a product containing two glucoses and one migrated benzoyl on the dodecanol arms) were isolated as a white solid. (Yield: 1.81 g, 0.73 mmol, 76%). ^{1}H NMR (400 MHz, $CDCl_3$, HH-COSY, HSQC): δ 8.37 (s, 3H, CH_{arom}), 8.04 – 7.99 (m, 6H, H_{arom}), 7.98 – 7.93 (m, 6H, H_{arom}), 7.93 – 7.87 (m, 6H, H_{arom}), 7.87 – 7.80 (m, 6H, H_{arom}), 7.58 – 7.44 (m, 9H, H_{arom}), 7.44 – 7.23 (m, 27H, H_{arom}), 6.61 (t, *J* = 5.3 Hz, 3H, NH), 5.92 (t, *J* = 9.7 Hz, 3H, H-3), 5.68 (t, *J* = 9.7 Hz, 3H, H-4), 5.53 (dd, *J* = 9.8, 7.9 Hz, 3H, H-2), 4.85 (d, *J* = 7.9 Hz, 3H, H-1), 4.64 (dd, *J* = 12.1, 3.2 Hz, 3H, H-6a), 4.51 (dd, *J* = 12.1, 5.2 Hz, 3H, H-6b), 4.21 – 4.13 (m, 3H, H-5), 3.91 (dt, *J* = 9.7, 6.3 Hz, 3H, C*H*H-*O*), 3.54 (dt, *J* = 9.7, 6.7 Hz, 3H, CH*H*-*O*), 3.43 (q, *J* = 6.7 Hz, 6H, CH_2-*N*), 1.64 – 1.45 (m, 12H, CH_2 (6x)), 1.39 – 0.98 (m, 48H, CH_2 (24x)); ^{13}C NMR (101 MHz, $CDCl_3$, HSQC): δ 166.3, 165.9, 165.7, 165.3, 165.2, 135.4, 133.5, 133.3, 133.3, 133.2, 129.9, 129.8, 129.8, 129.7, 129.6, 129.4, 128.9, 128.9, 128.5, 128.4, 128.4, 128.4, 128.1, 101.4, 73.0, 72.2, 72.0, 70.5, 69.9, 63.3, 40.5, 30.4, 29.6, 29.6, 29.6, 29.6, 29.5, 29.5, 29.4, 29.3, 27.1, 25.9.

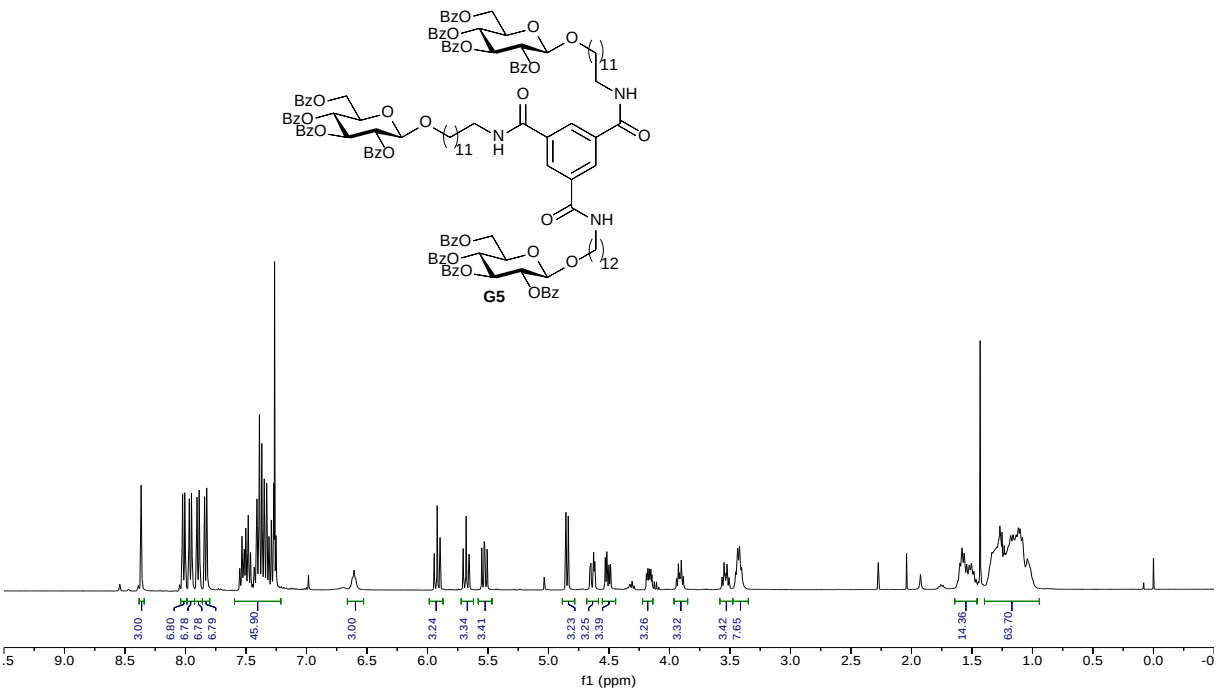
G5
3.00
6.80
6.78
6.78
6.79
45.90
3.00
3.24
3.34
3.41
3.23
3.25
3.39
3.26
3.32
3.42
7.65
14.36
63.70
f1 (ppm)

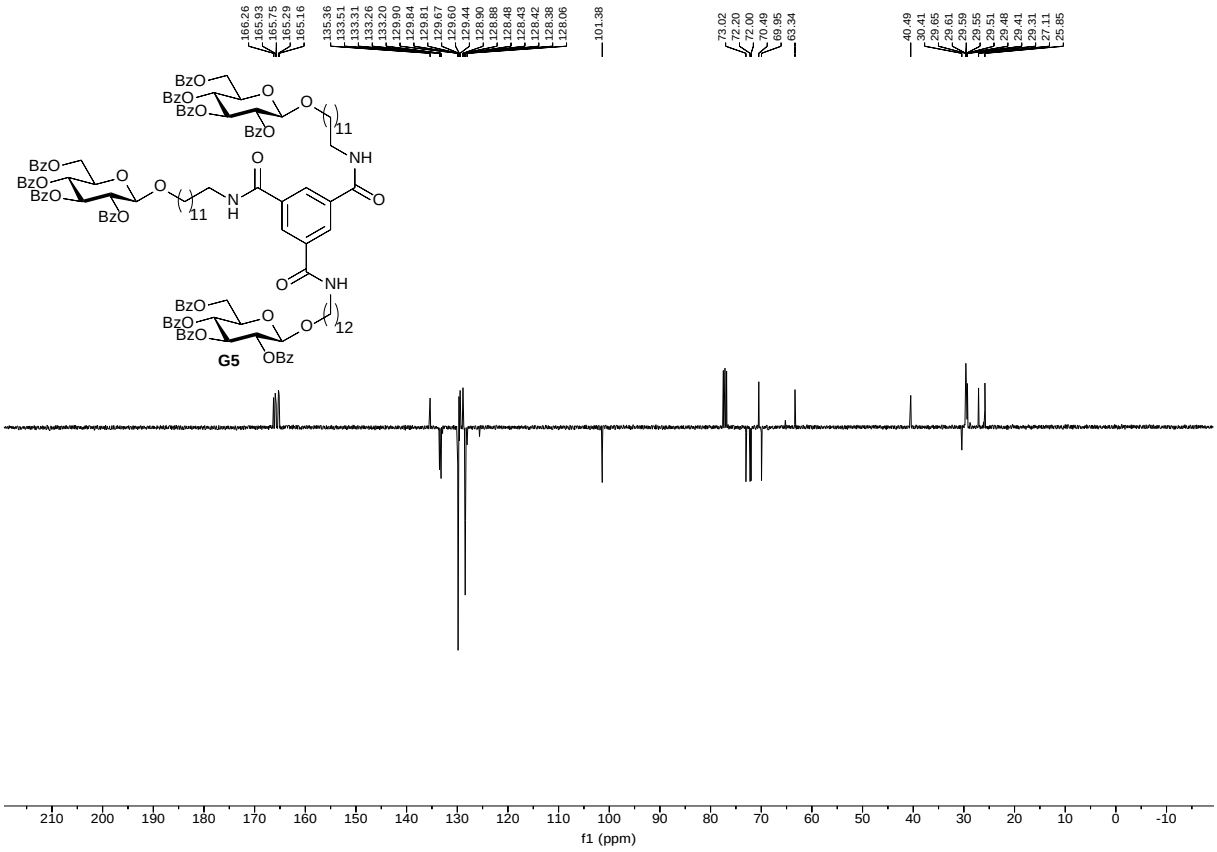
G5
f1 (ppm)

***N*^{1}, *N*^{3}, *N*^{5}-Tris(1-*O*-dodecyl-*β*-D-glucopyranoside)benzene-1,3,5-tricarboxamide**.

Compound **G5** (1.47 g, 0.59 mmol) was dissolved in a mixture of dioxane, t-BuOH and MeOH (17 mL, 0.035 M, 3/5/10, v/v/v), a solution of NaOMe was added (10 mL, 25% wt, 44 mmol, 75 eq) and the mixture was refluxed for three days. The mixture was quenched with Amberlite H^+ and concentrated. After purification by RP-HPLC (29-45 % ACN in 0.1% TFA in H_2O, 10 min, Linear gradient 5 mL/min, Develosil RPAQUEOUS 10.0 x 250 mm), BTA-Glc and BTA-2/3-glucose were isolated as a white powder after lyophilizing. (Yield product: BTA-Glc: 305 mg, 0.24 mmol, 41%) (Yield byproduct: BTA-2/3-glucose: 118.3 mg, 0.109 mmol, 18%).

2x Glucose: IR (cm^{-1}): 3318, 2919, 2852, 1639, 1594, 1538, 1433, 1294, 1076, 698; ^{1}H NMR (400 MHz, DMSO-*d*$_6$, COSY, HSQC) δ 8.65 (t, *J* = 5.4 Hz, 3H, NH), 8.36 (s, 3H, H_{arom}), 5.09 – 4.24 (m, 9H, OH), 4.08 (d, *J* = 7.8 Hz, 2H, H-1), 3.78 – 3.70 (m, 2H, C*H*H-O-Glc), 3.65 (d, *J* = 11.0 Hz, 2H, H-6a), 3.47 – 3.33 (m, 6H, CH*H*-O-Glc, H-6b, C*H*$_2$-OH), 3.26 (q, *J* = 6.5 Hz, 6H, C*H*$_2$-NH), 3.16 – 2.99 (m, 6H, H-3, H-4, H-5), 2.92 (t, *J* = 8.3 Hz, 2H, H-2), 1.59 – 1.44 (m, 10H, CH_2), 1.42 – 1.36 (m, 2H, CH_2), 1.36 – 1.18 (m, 48H, CH_2); ^{13}C NMR (101 MHz, DMSO-*d*$_6$, HSQC) δ 165.4, 135.1, 128.3, 102.9, 76.8, 76.8, 73.5, 70.1, 68.6, 61.1, 60.7, 32.6, 29.3, 29.1, 29.0, 28.9, 26.5, 25.6.

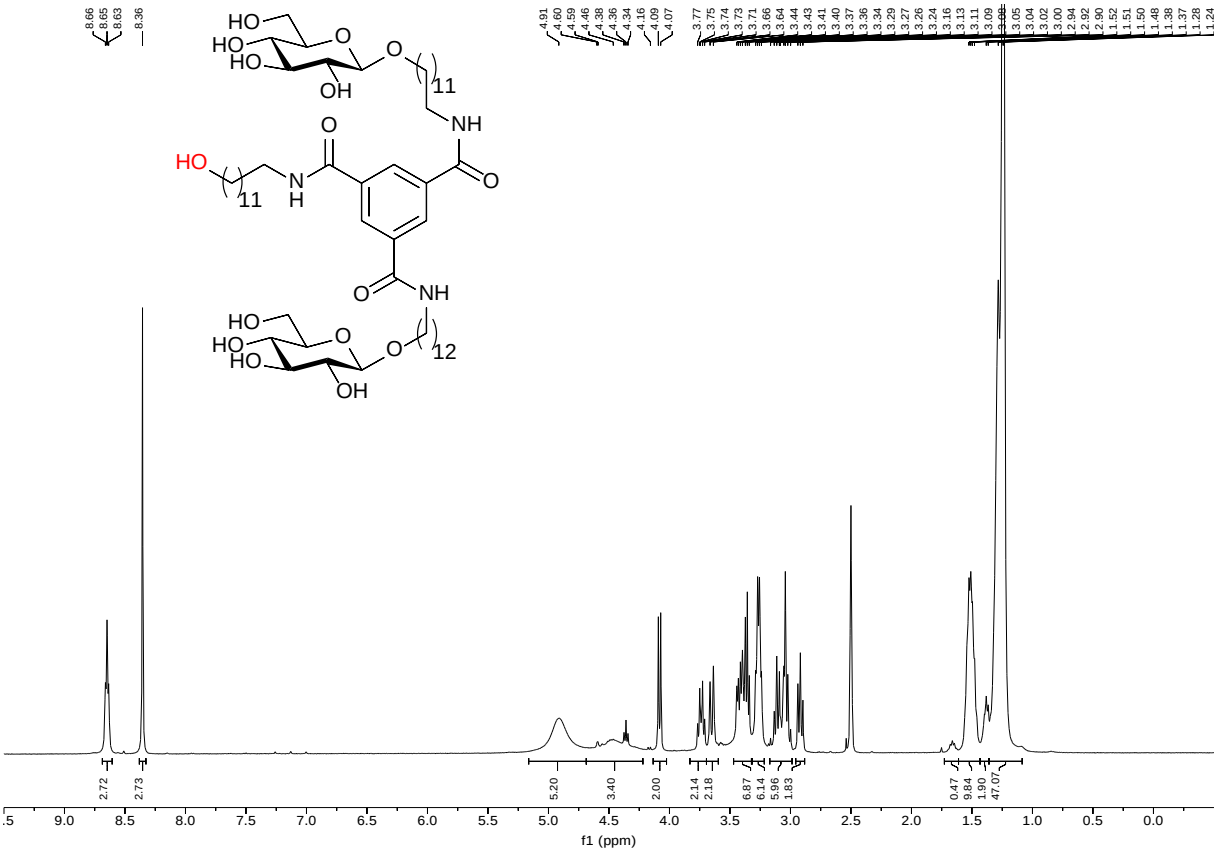
f1 (ppm)

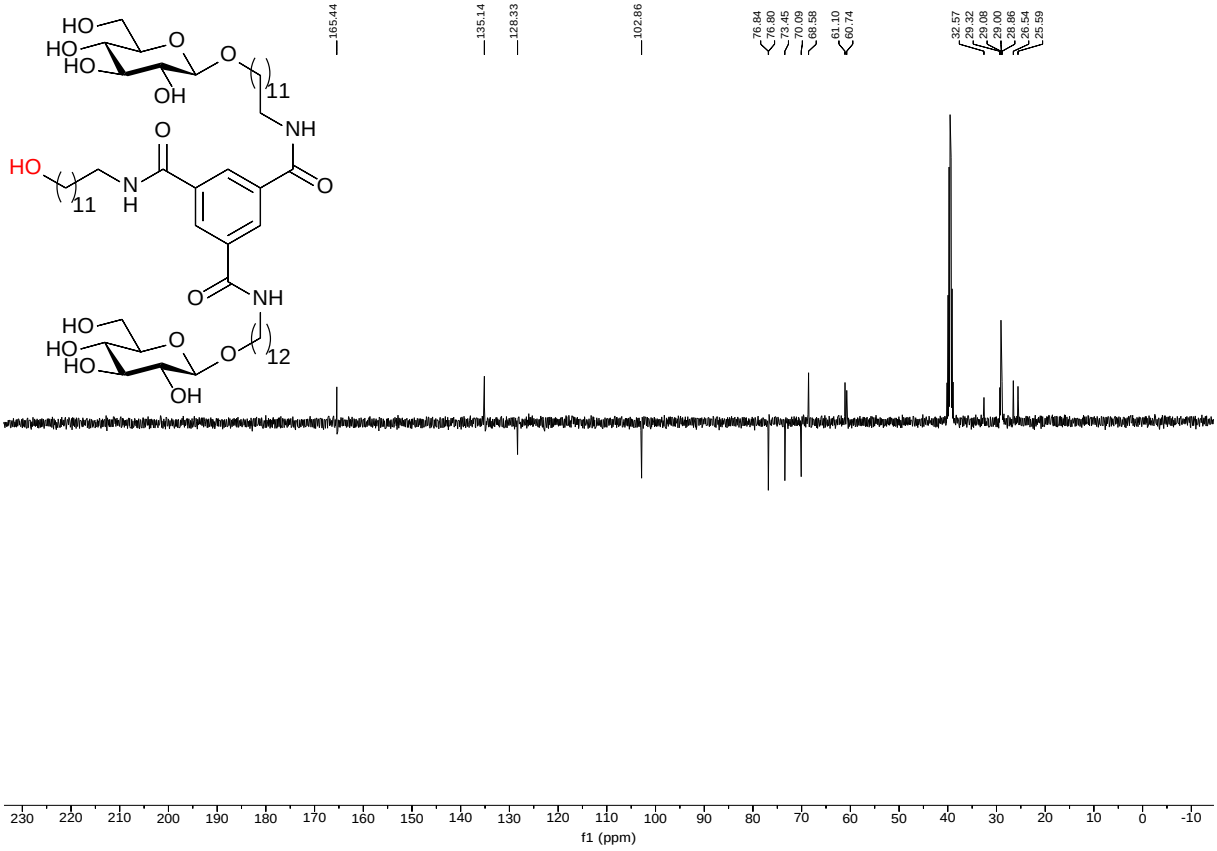
f1 (ppm)

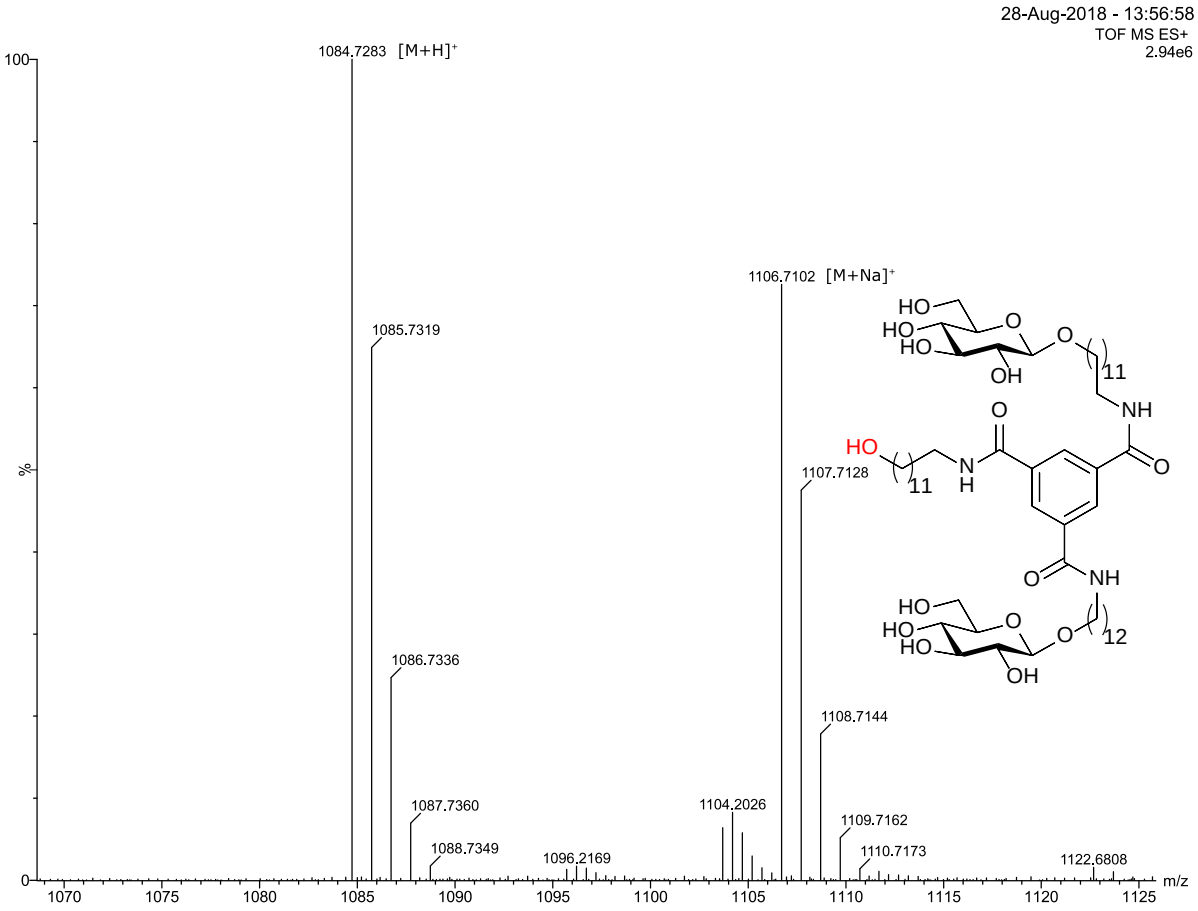

<u>3x Glucose:</u> IR (cm^{-1}): 3307, 2922, 2852, 1641, 1540, 1435, 1293, 1202, 1075, 800; ^{1}H NMR (400 MHz, DMSO-*d*$_6$, HH-COSY, HSQC): δ 8.65 (t, *J* = 5.5 Hz, 3H, NH), 8.35 (s, 3H, H_{arom}), 5.36 – 4.20 (m, 12H, OH), 4.08 (d, *J* = 7.8 Hz, 3H, H-1), 3.74 (dt, *J* = 9.4, 6.8 Hz, 3H, C*H*H-*O*), 3.69 – 3.61 (dd, *J* = 11.8, 1.4 Hz, 3H, H-6a), 3.47 – 3.35 (m, 6H, H-6b, CH*H*-*O*), 3.26 (q, *J* = 6.5 Hz, 6H, C*H*$_2$-NH), 3.19 – 2.97 (m, 9H, H-3, H-4, H-5), 2.92 (d, *J* = 7.9 Hz, 3H, H-2), 1.59 – 1.44 (m, 12H, CH_2 (6x)), 1.37 – 1.19 (m, 48H, CH_2 (24x)); ^{13}C NMR (101 MHz, DMSO-*d*$_6$, HSQC): δ 165.4 (C=O), 135.1 (C_q), 128.3 (CH_{arom}), 102.8 (C-1), 76.8, 76.8 (C3&C4/C5), 73.4 (C-2), 70.1 (C-4/C-5), 68.6 (CH_2-*O*), 61.1 (C-6), 39.5 (CH_2-*N*), 29.3, 29.1, 28.9, 26.5, 25.6 (CH_2). LCMS; *M*w_{calc} = 1246.58 g/mol, m/z_{obs} = 1246.75 $[M+H]^+$.

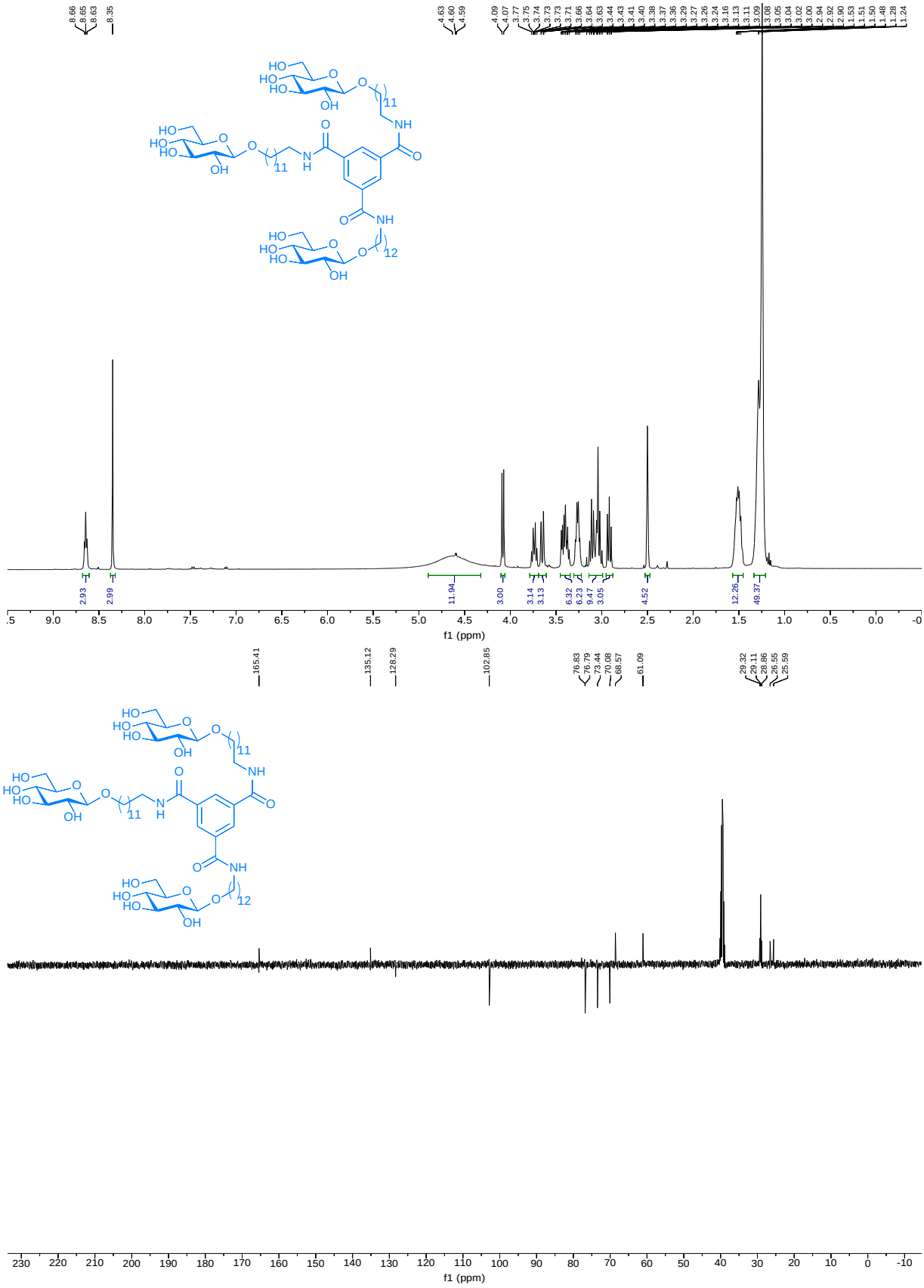
8.66
8.65
8.63
8.35
4.63
4.60
4.59
4.09
4.07
3.77
3.75
3.74
3.73
3.73
3.71
3.66
3.64
3.63
3.44
3.43
3.41
3.40
3.38
3.37
3.36
3.29
3.27
3.26
3.24
3.16
3.13
3.11
3.09
3.08
3.05
3.04
3.02
3.00
2.94
2.92
2.90
1.53
1.51
1.50
1.48
1.28
1.24
HO
HO
HO
O
OH
11
NH
O
N
H
12
2.93
2.99
11.94
3.00
3.14
3.13
6.32
6.23
9.47
3.05
4.52
12.26
49.37
f1 (ppm)
165.41
135.12
128.29
102.85
76.83
76.79
73.44
70.08
68.57
61.09
29.32
29.11
28.86
26.55
25.59

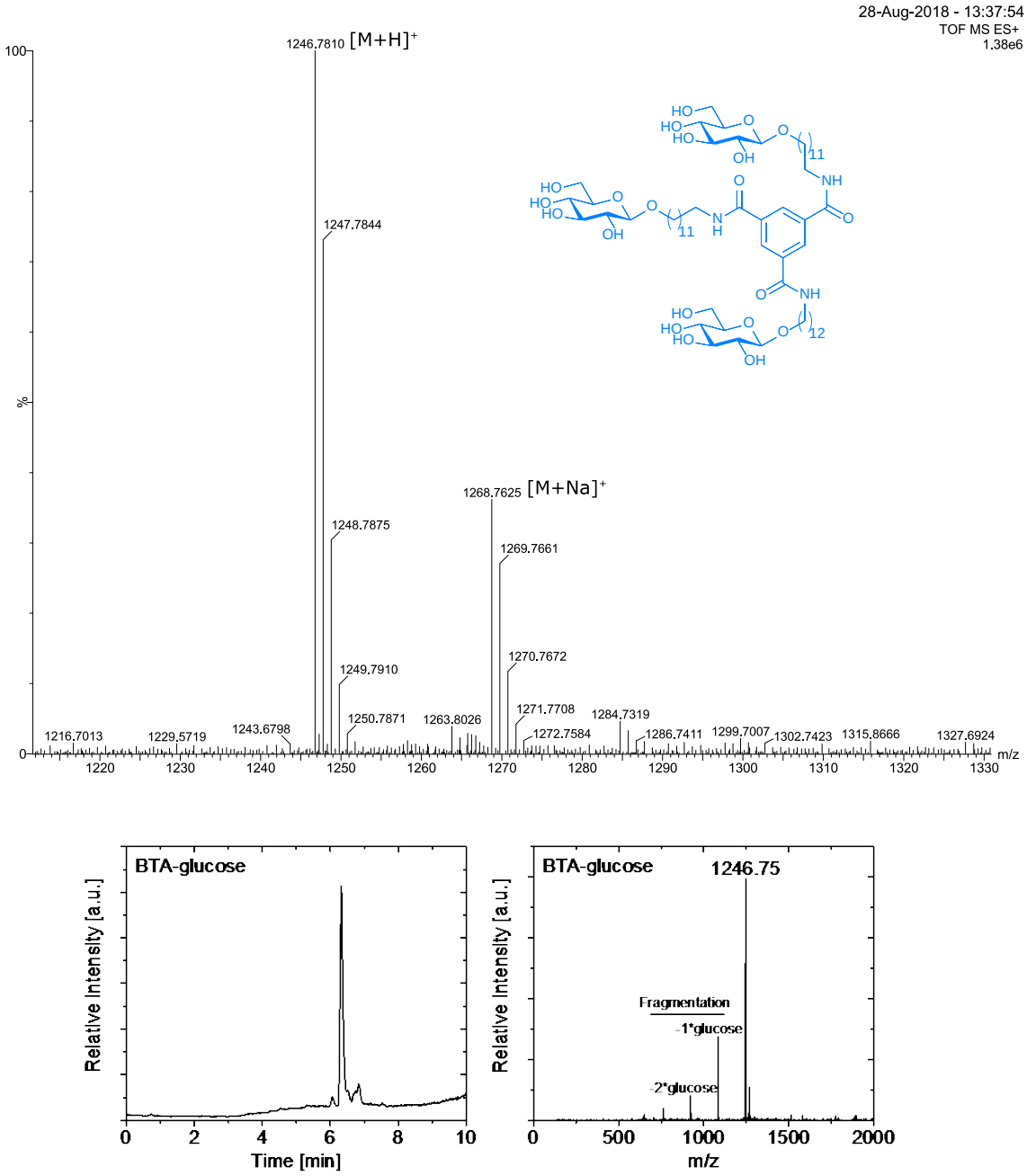

Figure S21: ^{1}H NMR, ^{13}C NMR, MALDI-TOF and LCMS spectra of BTA-Glc. LCMS, Left: Total ion current (TIC) chromatogram of analytical reversed phase-high performance liquid chromatography (RP-HPLC) with a gradient of 5-100% acetonitrile over a course of 10 minutes, Right: Electrospray ionization-mass spectrometry (ESI-MS) m/z spectrum.

Synthesis of BTA-Cel

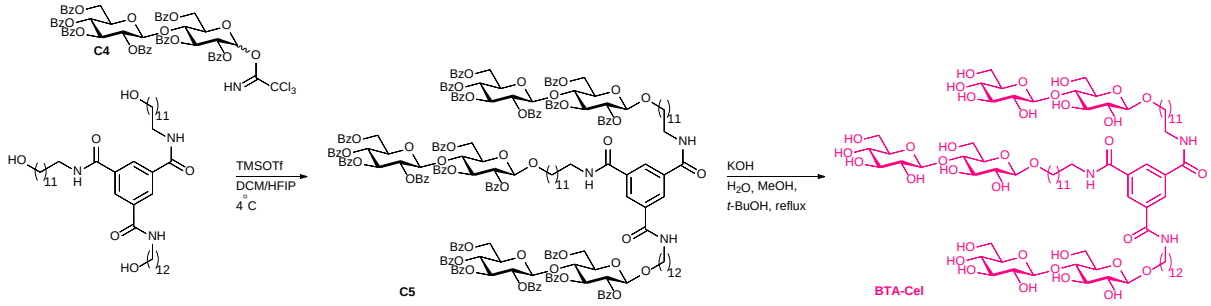

Scheme S3: Synthetic approach to **BTA-Cel**.

***N*^{1}, *N*^{3}, *N*^{5}-Tris(4-*O*-(2,3,4,6-tetra-*O*-benzoyl-*β*-D-glucopyranoside)-2,3,6-tri-*O*-benzoyl-1-dodecyl-*β*-D-glucopyranoside)-benzene-1,3,5-tricarboxamide (C5)**.

Acceptor **BTA-OH** (1.33 g, 1.75 mmol, 1 eq) and 4-*O*-(2,3,4,6-tetra-*O*-benzoyl-β-D-glucopyranoside)-2,3,6-tri-*O*-benzoyl-α,β-D-glucopyranosyl trichloroacetimidate[4] (10.66 g, 8.77 mmol, 5 eq) were combined and co-evaporated 3x with toluene under N_2 atmosphere. The reaction mixture was dissolved in DCM/HFIP (76 mL, 0.023 M, 4/1, v/v) and flame dried molecular sieves (3Å) were added and the mixture was stirred at r.t. for 30 min, after which it was cooled to 0 ˚C. TfOH (155 µL, 1.75 mmol, 1 eq) was added dropwise and the mixture was stirred at 4 ˚C overnight after which it was quenched with Et_3N (0.5 mL) diluted in DCM and washed with $NaHCO_3$ (sat aq. 3x). The organic layer was dried over $MgSO_4$, filtered and concentrated. After purification by silica gel column chromatography (1/1 EtOAc/PE, v/v) compound **C5** was isolated as a white powder. (Yield: 3.46 g, 0.88 mmol, 50%). ^{1}H NMR (400 MHz, $CDCl_3$, HH-COSY, HSQC): δ 8.35 (s, 3H, $H_{arom\ BTA}$), 8.01 – 7.88 (m, 30H, H_{arom}), 7.78 – 7.71 (m, 12H, H_{arom}), 7.60 – 7.16 (m, 63H, H_{arom}), 6.49 (d, *J* = 5.4 Hz, 3H, NH), 5.83 – 5.67 (m, 6H, H-3, H-3’), 5.51 (dd, *J* = 9.8, 7.9 Hz, 3H, H-2’), 5.45 – 5.33 (m, 6H, H-2, H-4’), 4.93 (d, *J* = 7.9 Hz, 3H, H-1’), 4.64 (d, *J* = 7.9 Hz, 3H, H-1), 4.61 (dd, *J* = 11.7, 1.8 Hz, 3H, H-6a), 4.45 (dd, *J* = 12.1, 4.5 Hz, 3H, H-6b), 4.23 (t, *J* = 9.4 Hz, 3H, H-4), 4.05 (dd, *J* = 11.9, 2.9 Hz, 3H, H-6a’), 3.87 – 3.66 (m, 12H, H-5, H-5’, H-6b’, C*H*H-*O*), 3.50 – 3.33 (m, 9H, CH*H*-*O*, CH_2-*N*), 1.66 – 0.91 (m, 60H, CH_2); ^{13}C NMR (101 MHz, $CDCl_3$, HSQC): δ 165.9, 165.8, 165.7, 165.5, 165.3, 165.1, 164.8 (C=O), 135.3 (C_q), 133.5, 133.4, 133.2, 129.9, 129.8, 129.7 (CH_{arom}), 129.6, 129.5, 128.7, 128.7 (C_q), 128.6, 128.6, 128.6, 128.4, 128.4, 128.4 (CH_{arom}), 101.1, 101.0 (C-1,C-1’), 76.6 (C-4), 73.1, 72.9 (C-3, C-3’), 72.5 (C-5, C-5’), 72.0, 70.4 (C-2, C-2’), 69.5 (CH_2-*O*), 62.7, 62.6 (C-6, C-6’), 40.5 (CH_2-*N*), 29.6, 29.6, 29.5, 29.4, 29.3, 27.1, 25.8 (CH_2).

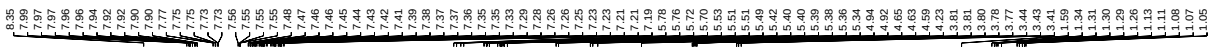

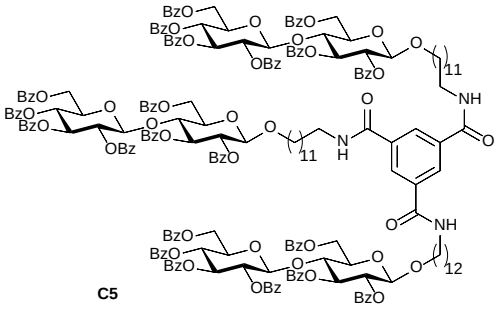
C5

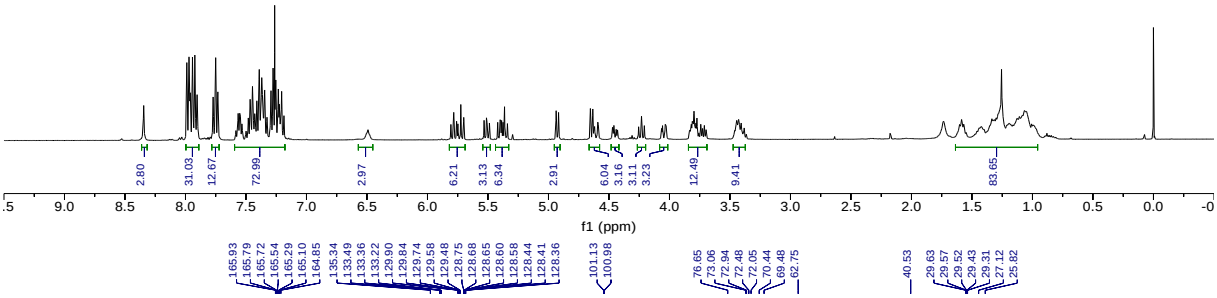
f1 (ppm)

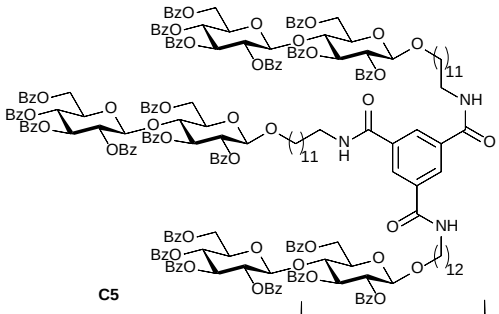
C5

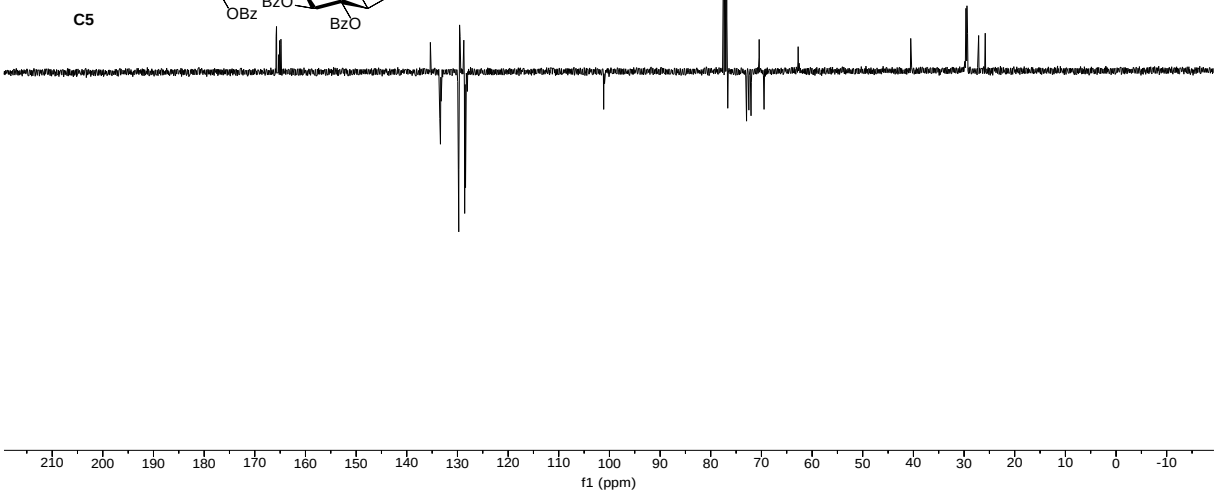
f1 (ppm)

***N*^{1}, *N*^{3}, *N*^{5}-Tris(4-*O*-*β*-D-glucopyranoside-1-dodecyl-*β*-D-glucopyranoside)-benzene-1,3,5-tricarboxamide**.

Compound **C5** (3.46 g, 0.88 mmol) was dissolved in a mixture of water, MeOH, t-BuOH (65 mL, 1/6/6, v/v/v) to which KOH (15 mL, 1 M, aq., 15 mmol, 17eq) was added dropwise after which the mixture was refluxed for three days after which it was neutralized with acetic acid, and purified over C18 (0 – 20% ACN in H_2O).

^{1}H NMR (400 MHz, Methanol-d_4 HH-COSY, HSQC): δ 8.35 (s, 3H), 4.39 (d, *J* = 7.8 Hz, 3H), 4.25 (d, *J* = 7.8 Hz, 3H), 3.92 – 3.76 (m, 12H), 3.70 – 3.16 (m, 36H), 1.67 – 1.54 (m, 12H), 1.44 – 1.21 (m, 48H); ^{13}C NMR (101 MHz, MeOD, HSQC): δ 136.8, 129.8, 104.6, 104.1 (C-1), 80.7, 78.0, 77.8, 76.4, 76.4, 74.9, 74.8, 71.3, 70.9, 62.4, 61.8, 49.6, 41.2, 30.7, 30.6, 30.5, 28.1, 27.1; LCMS; Mw_{calc} = 1732.00, m/z_{obs} = 1732.25 $[M+H]^+$;

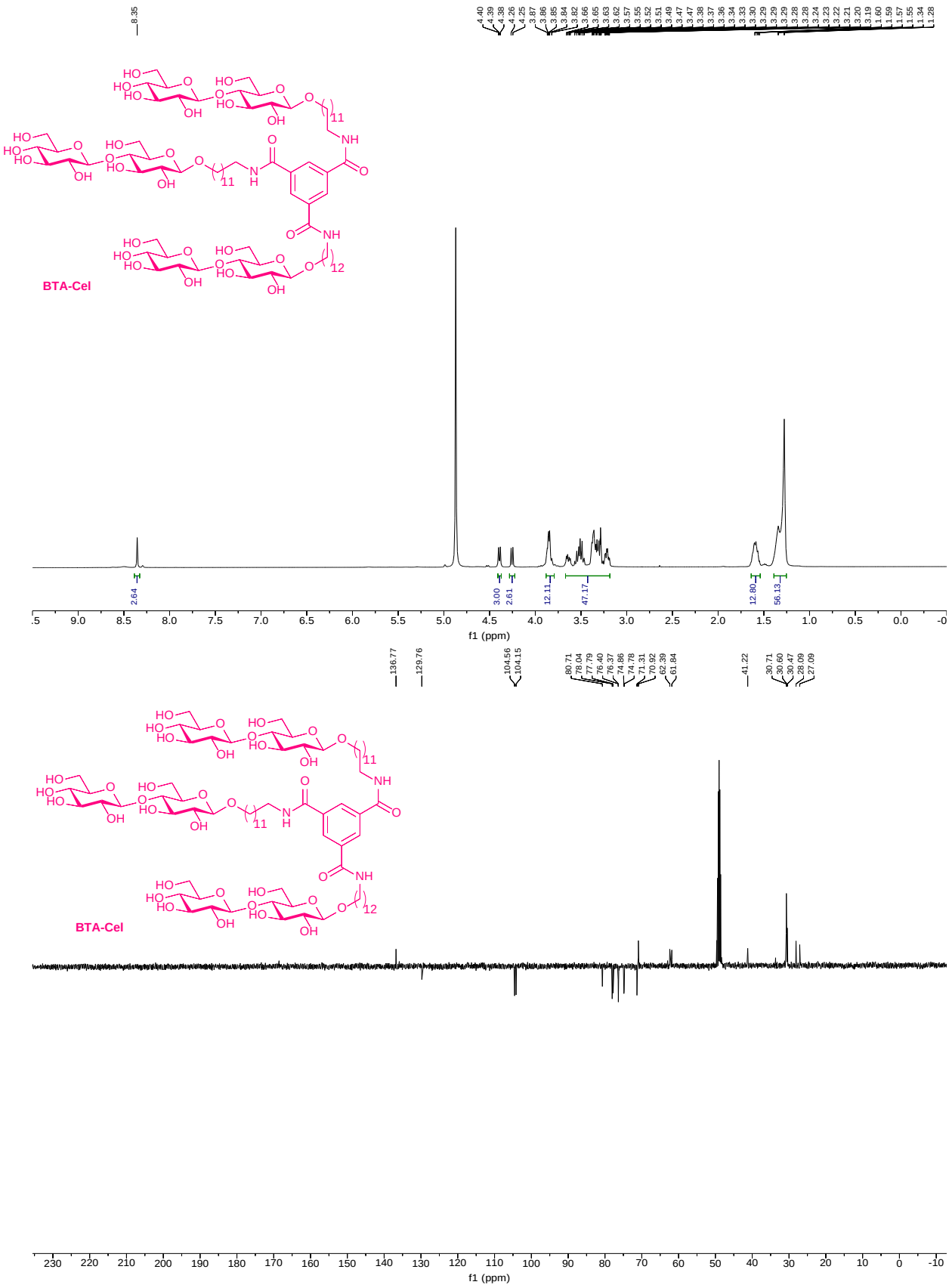
BTA-Cel
f1 (ppm)
BTA-Cel
f1 (ppm)

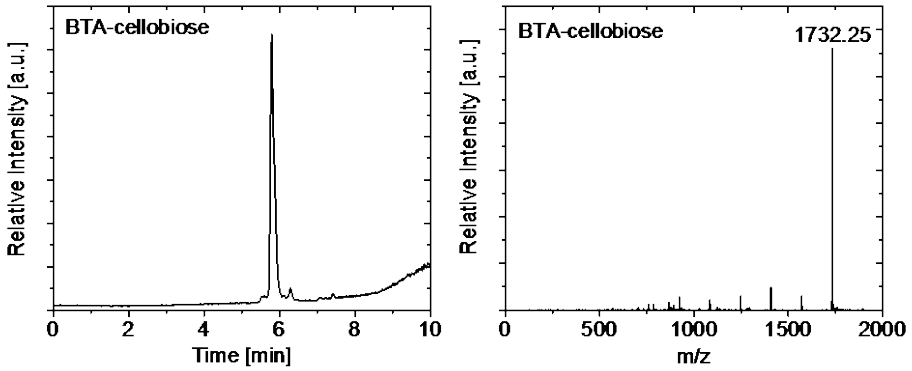

Figure S22: ^{1}H NMR, ^{13}C NMR, and LCMS spectra of BTA-Cel. LCMS, Left: Total ion current (TIC) chromatogram of analytical reversed phase-high performance liquid chromatography (RP-HPLC) with a gradient of 5-100% acetonitrile over a course of 10 minutes, Right: Electrospray ionization-mass spectrometry (ESI-MS) m/z spectrum.

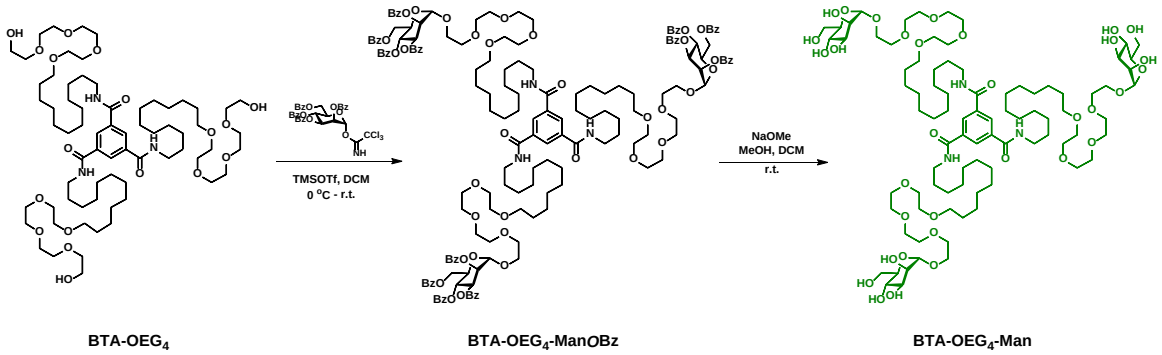

Scheme S4: Synthetic approach to **BTA-OEG$_4$-Man**.

N^1, *N*^{3}, *N*^{5}-Tris(dodecyl-tetra(ethylene glycol)-*O*-α-D-mannopyranoside)benzene-1,3,5-tricarboxamide

An oven-dried RB flask containing a stir bar and 4 Å molecular sieves was charged with 2,3,4,6-tetra-*O*-benzoyl-α-D-mannopyranosyl trichloroacetimidate[3] (594.1 mg, 803.8 µmol), BTA-EG$_4$ (258.8 mg, 200.9 µmol) and dry dichloromethane (DCM, 6 mL). The mixture was stirred at 0 °C for 30 min under an Ar atmosphere. To the mixture, trimethylsilyl trifluoromethanesulfonate (TMSOTf, 20.8 µL, 120 µmol) in DCM (2 mL) was added dropwise over 5 min. Progress was monitored by TLC (DCM/MeOH = 49:1) and the reaction was quenched with trimethylamine after 30 min. After the mixture was first warmed to r.t. and then concentrated, the crude material was used for next step without further purification.

To a solution of BTA-EG$_4$-Man*O*Bz dissolved in dry DCM (2 mL) and methanol (MeOH, 8 mL) under Ar at r.t., sodium methoxide (172.2 mg, 3.185 mmol, 1 *eqv*. to *O*Bz group) was added while stirring. Progress was monitored by TLC and the reaction was quenched with Dowex® 50WX8 hydrogen form resin after 2 h. The resin was removed by filtration and the filtrate was concentrated under reduced pressure. The crude product was purified by reversed-

phase chromatography (H_2O/MeOH gradient 50/50–20/90 v/v) to give **BTA-EG$_4$-Man** as a white, fluffy solid after lyophilization (199.6 mg, 56% in two steps).
^{1}H NMR (400 MHz, CD_3OD) δ ppm 8.60 (t, *J* = 5.7 Hz, 3H), 8.37 (s, 3H), 4.79 (d, *J* = 1.7 Hz, 3H), 3.88 – 3.53 (m, 66H), 3.48 (t, *J* = 1.7 Hz, 6H), 3.43 – 3.32 (m, 6H), 1.60 (dp, *J* = 34.8, 6.9 Hz, 12H), 1.44 – 1.27 (m, , 48H).
^{13}C NMR (101 MHz, CD_3OD) δ ppm 167.23, 135.48, 128.35, 100.36, 73.22, 71.17, 70.98, 70.72, 70.22, 70.19, 70.16, 70.00, 69.76, 67.23, 66.37, 61.57, 39.82, 29.33, 29.29, 29.18, 29.06, 26.69, 25.81.
FT-IR (cm^{-1}): 3380, 3248, 3073, 2912, 2851, 1724, 1639, 1558, 1467, 1351, 1295, 1251, 1094, 976, 881, 808, 721.
MALDI-TOF-MS: Calculated for $C_{87}H_{159}O_{33}N_3Na^+$ $[M+Na]^+$ 1797.08; found, 1797.09.

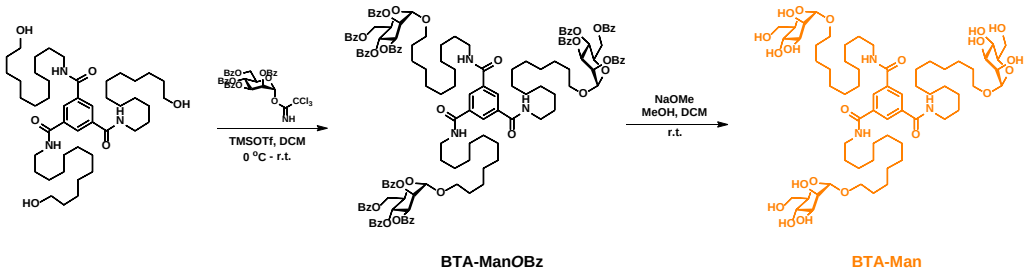

Scheme S5: Synthetic approach to **BTA-Man**.

***N*^{1}, *N*^{3}, *N*^{5}-Tris(dodecyl-*O*-α-D-mannopyranoside)benzene-1,3,5-tricarboxamide**
An oven-dried RB flask containing a stir bar and 4 Å molecular sieves was charged with 2,3,4,6-tetra-*O*-benzoyl-α-D-mannopyranosyl trichloroacetimidate (911.9 mg, 1.234 mmol), **BTA-OH** (234.5 mg, 308.5 µmol) and dry CH_2Cl_2 (10 mL). The mixture was stirred at 0 °C for 30 min under an Ar atmosphere. To the mixture, trimethylsilyl trifluoromethanesulfonate (TMSOTf, 20.8 µL, 120 µmol) in DCM (2 mL) was added dropwise over 5 min. Progress was monitored by TLC (DCM/MeOH = 49:1) and the reaction was quenched with Et_3N after 16 h. After the mixture was first warmed to r.t. and then concentrated, the crude material was used for next step without further purification.
To a solution of BTA-Man*O*Bz dissolved in dry DCM (2 mL) and methanol (MeOH, 8 mL) under Ar at r.t., sodium methoxide (266.5 mg, 4.936 mmol, 1 *eqv*. to *O*Bz group) was added while stirring. Progress was monitored by TLC and the reaction was quenched with Dowex® 50WX8 hydrogen form resin after 2 h. The resin was removed by filtration and the filtrate was concentrated under reduced pressure. The crude product was purified by reversed-phase chromatography (H_2O/MeOH gradient 50/50–20/80 v/v) to give **BTA-Man** as a white, fluffy solid after lyophilization (172.6 mg, 45% in two steps).
^{1}H NMR (400 MHz, CD_3OD) δ ppm 8.36 (s, 3H), 4.72 (d, *J* = 1.7 Hz, 3H), 3.86 – 3.65 (m, 15H), 3.60 (t, J = 9.5 Hz, 3H), 3.51 (ddd, *J* = 9.5, 5.6, 2.4 Hz, 3H), 3.45 – 3.33 (m, 9H), 1.61 (m, *J* = 25.0, 6.8 Hz, 12H), 1.44 – 1.25 (m, 48H).
^{13}C NMR (101 MHz, CD_3OD) δ ppm 167.27, 135.48, 128.32, 100.14, 73.17, 71.28, 70.90, 67.24, 67.17, 61.54, 39.82, 29.31, 29.28, 29.22, 29.15, 29.05, 26.69, 25.95.

FT-IR (cm^{-1}): 3303, 2912, 2852, 1739, 1644, 1538, 1435, 1292, 1131, 1057, 976, 812, 689.
MALDI-TOF-MS: Calculated for $C_{63}H_{111}O_{21}N_3Na^+$ $[M+Na]^+$ 1268.76; found, 1268.80.

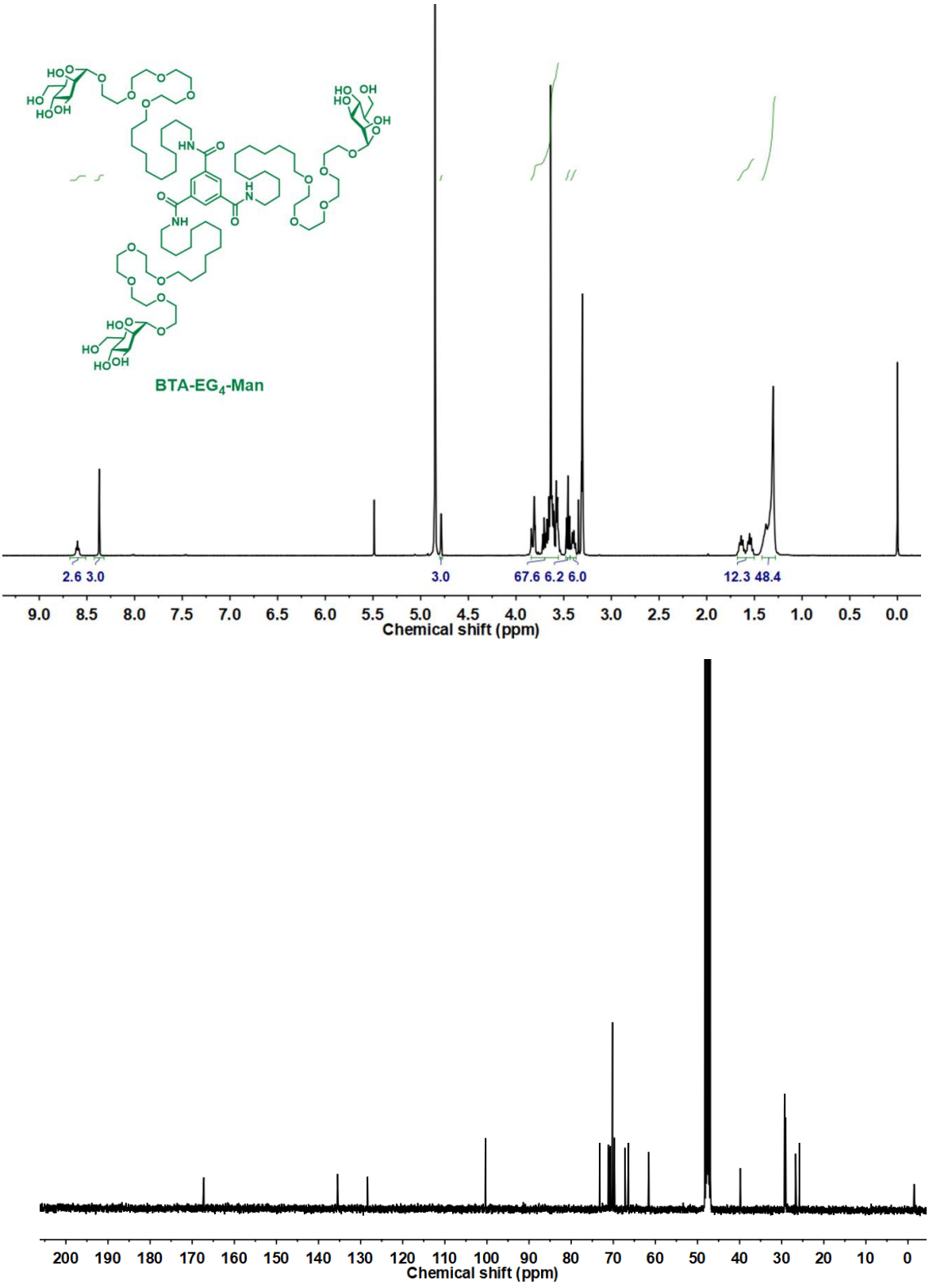

Figure S23: Top: ^{1}H NMR of **BTA-OEG$_4$-Man** in CD_3OD (400 MHz). Bottom: ^{13}C NMR of **BTA-OEG$_4$-Man** in CD_3OD (101 MHz)

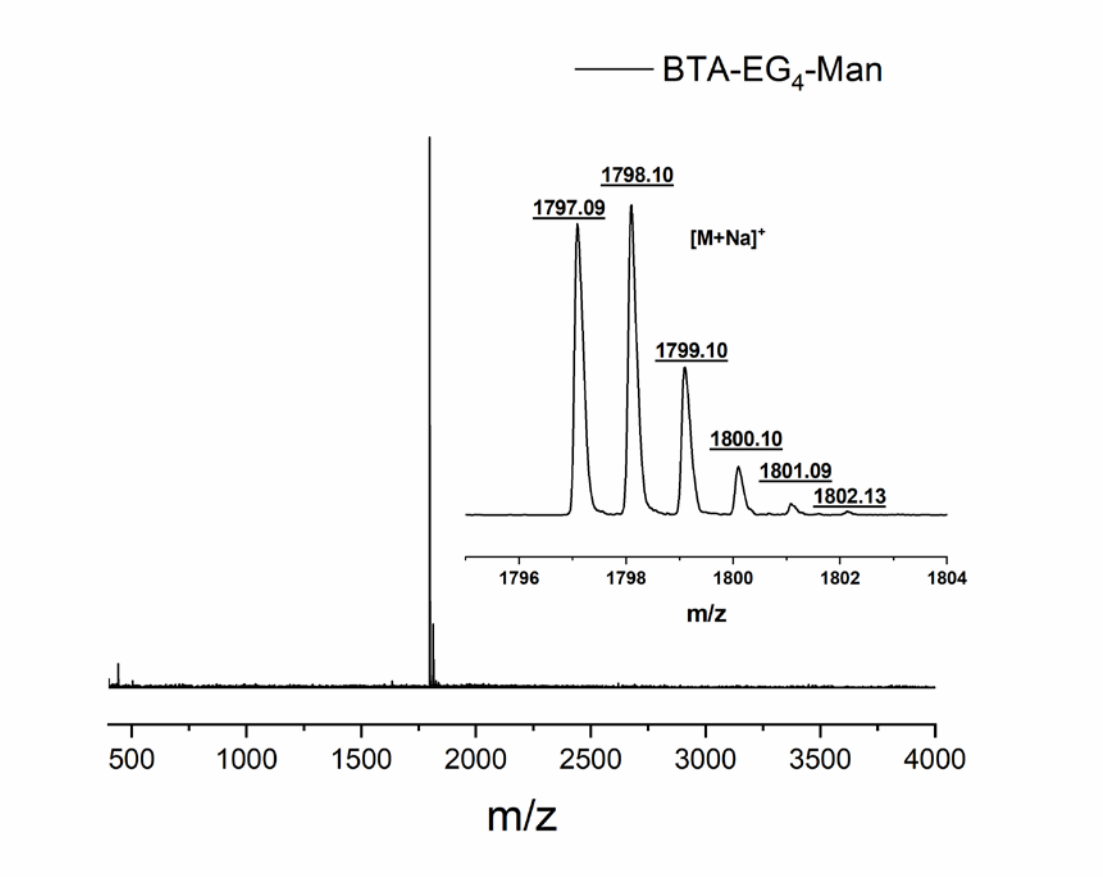

Figure S24: MALDI-TOF MS of **BTA-OEG$_4$-Man**

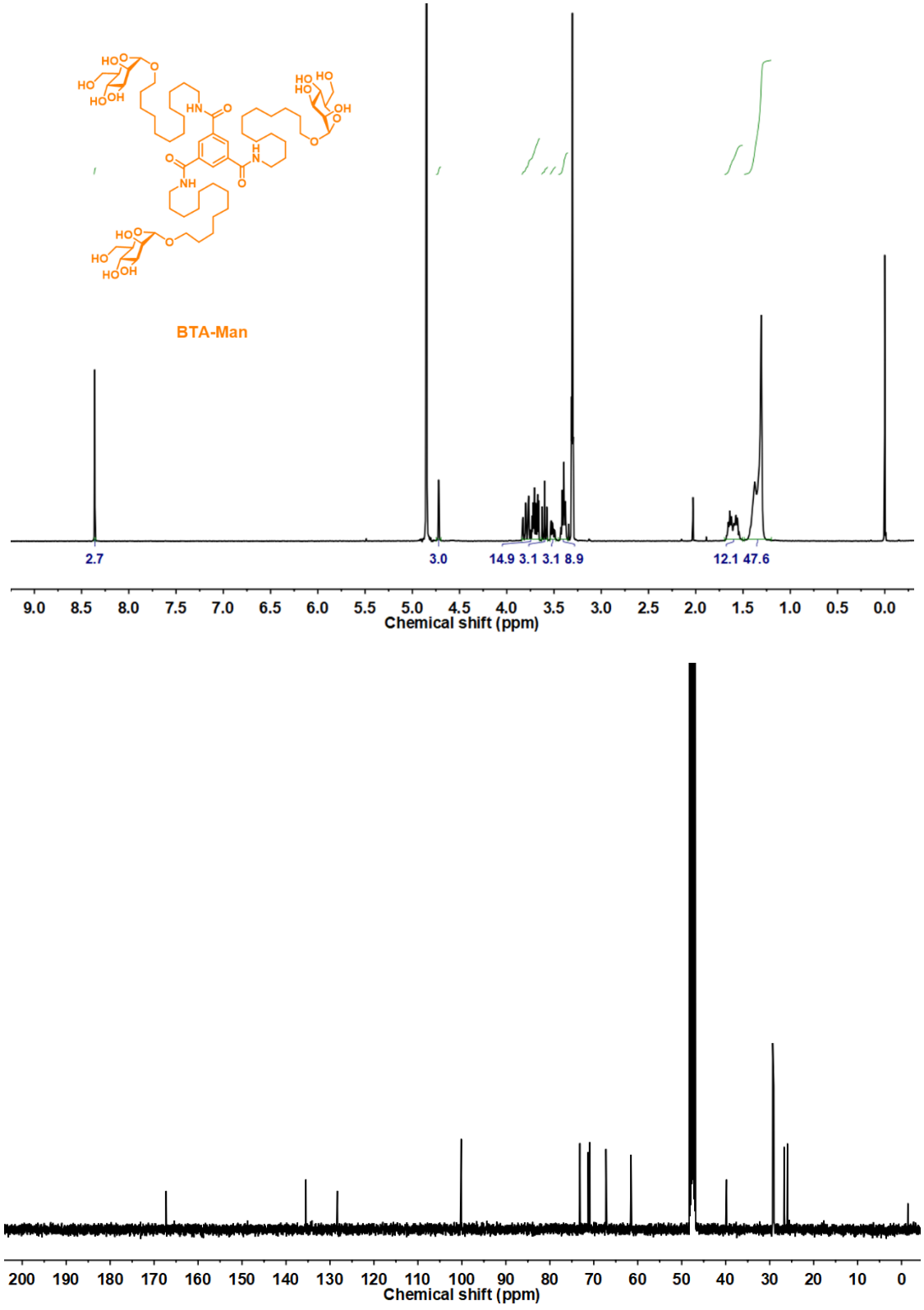

Figure S25: Top: ^{1}H NMR of **BTA-Man** in CD_3OD (400 MHz). Bottom: ^{13}C NMR of **BTA-Man** in CD_3OD (101 MHz)

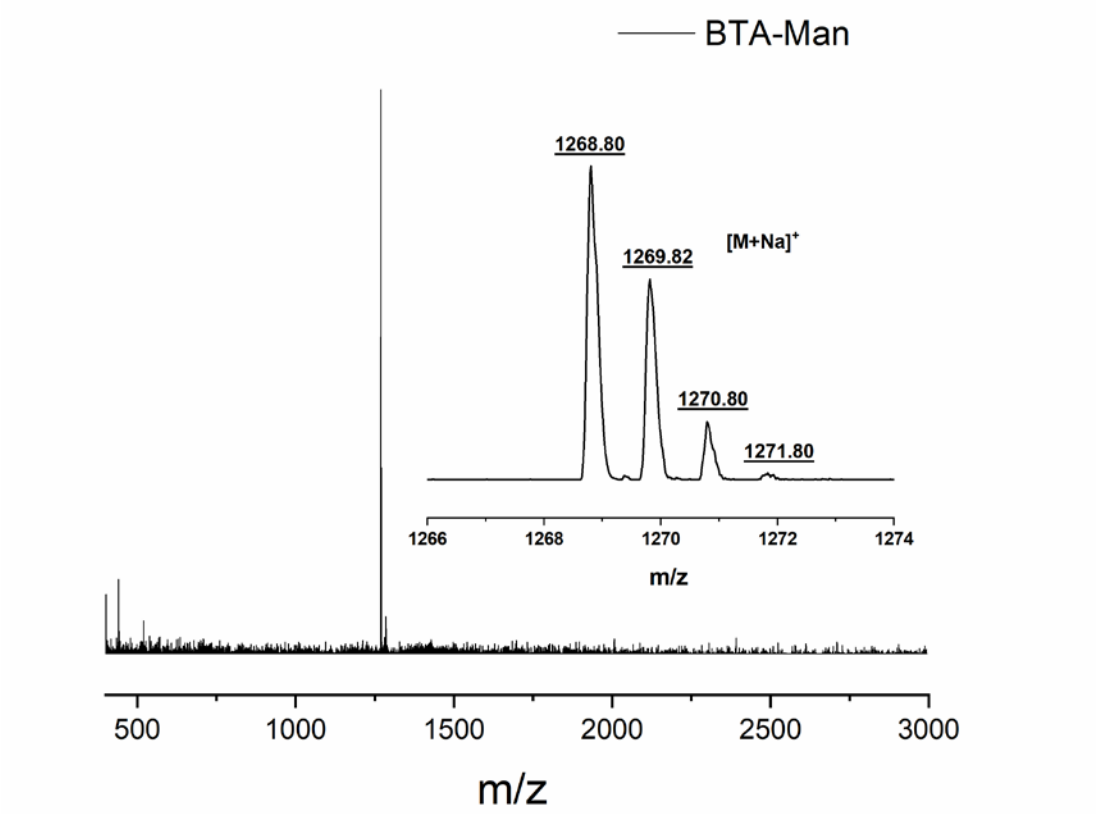

Figure S26: MALDI-TOF MS of **BTA-Man**

3. Methods

Self-assembly protocol for BTAs. BTA-Glc, BTA-Cel, BTA-OEG_4-Man or BTA-OEG_4 was weighed and dissolved in MQ water to yield in the predetermined concentration (50, 250, or 500 µM). The samples were vortexed for 10 seconds, and subsequently heated and stirred for 15 minutes at 80 °C. The samples were vortexed for another 10 seconds and allowed to self-assemble overnight at room temperature.

However, the above protocol was not applicable for the BTA-Man due to the strong carbohydrate-carbohydrate interactions. Therefore, injection from a co-solvent was applied. Briefly, BTA-Man was dissolved in methanol to obtain the concentrated stock solution, which was subsequently injected into MQ water (1 vol% of methanol) and allowed to equilibrate overnight, followed by dialysis against MQ water to remove methanol and generate the predetermined concentration (50, 250, or 500 µM) of BTA-Man solution.

Co-assembly protocol. Co-assembled samples were prepared by allowing the individual stocks to cool down to room temperature for 10 minutes after heating the stocks for 10 minutes at 80 °C as previously described. The mixtures 1:1, 2:1 and 1:2 were prepared by pipetting the correct amounts together. The samples were vortexed for 10 seconds, heated for another 10 minutes at 80 °C, vortexed for 10 seconds, and allowed to equilibrate at room temperature overnight before measuring.

UV and CD measurements. UV-vis and CD measurements were performed on samples with a 50 µM concentration using a 1 cm cuvette and with a concentration of 250 µM using a 1 mm cuvette. During the temperature interval measurements, the samples were equilibrated for 16 minutes before measuring, and due to the multi-scan mode the 5 samples at the designated temperature were measured within 26 minutes. LD was measured of the samples of each condition as well. Conditions with a significant LD effect were removed (BTA-OEG_4). The molar ellipticity ($\Delta\varepsilon$) of the CD intensity was calculated using the following equation $\Delta\varepsilon$=CD[mDeg] / c[M] * L[cm] * 32980.

Nile red assay. A dilution series was prepared followed by the addition of 1 µl of a 2.5 mM Nile red stock to 499 µl sample, to yield in a probe concentration of 5 µM. The samples were incubated for at least 30 minutes before measurement and protected from light.

SLS measurements. Samples were prepared at a 250 µM or 500 µM concentration and the scattering intensity was recorded at an angle of 40 to 130°. The data was processed using After ALV software, where the runs with irregular and peaked count rate profiles were removed (dust). The count rates were corrected for a difference in volume upon different angles by multiplying the count rate with the $\sin(\pi*\theta/180)$. The data was averaged per angle and the standard deviation was calculated.

SAXS measurements. Samples were prepared at a 500 μM concentration and the scattering intensity was recorded with a synchrotron beamline. The data was fitted in SasView using a cylinder or flexible cylinder model.

HDXMS measurements. Upon dilution 100 times of a stock BTA-saccharide solution (500 μM or 250 μM BTA-Man) in D_2O, all the OH groups of the saccharide moieties will immediately be exchanged with D_2O. There are 12 such OH groups for BTA-Glc, BTA-man and BTA-OEG_4-Man, and 21 for BTA-Cel. Because of the presence of the tiny amount of H_2O (1%), not all the OH groups will be transferred into OD. For example, in addition to 12D-BTA3NH for BTA-man, there is statistically about 12% of 11D-BTA3NH relative to 12D-BTA3NH while the presence of 10D-BTA3NH is negligible. Obviously, the signal intensity corresponding to the total amount of the un-exchanged BTA3NH is the sum of peak intensities of 11D-BTA3NH and 12D-BTA3NH including all their corresponding isotopes, which can be calculated by

$$M_0 = A_{11D}(1 + \sum_{i=2}^{n} j_{i,0}) + (A_{12} - A_{11} \times j_{2,0})(1 + \sum_{i=2}^{n} j_{i,0}) \quad (1)$$

Where A_{11D} and A_{12D} are the signal intensities for the peaks with the monoisotopic mass of 11D-BTA3NH and 12D-BTA3NH respectively, and $j_{i,0}$ is the theoretical relative intensities of other isotopes to the monoisotopic peaks. For the monoisotopic peak, $j_{1,0}$ is arbitrarily set at $j_{1,0} = 1$. The percentages of un-exchanged BTA3NH for BTA-Glc, BTA-man and BTA-OEG_4-Man were calculated by the following formula

$$BTA3NH = \frac{Mo}{\sum_{i=11}^{n} A_{iD}} * 100 \quad (2)$$

Similarly, for BTA-Cel

$$M_0 = A_{20D}(1 + \sum_{i=2}^{n} j_{i,0}) + (A_{21} - A_{20} \times j_{2,0})(1 + \sum_{i=2}^{n} j_{i,0}) \quad (3)$$

$$BTA3NH = \frac{Mo}{\sum_{i=20}^{n} A_{iD}} * 100 \quad (4)$$

Subsequently, the data was fitted with a triexponential fit, following the equation:

$$y = A * \exp(-t * C) + B * \exp(-t * D) + E * \exp(-t * F) \quad (5)$$

Fitted equations:

BTA-OEG_4

y = 44.04*exp(-t*0.005)+42.24*exp(-t*29.74)+13.67*exp(-t*2.60) Adj. R^2=0.99872

BTA-Man

y = 49.96*exp(-t*0.002)+16.19*exp(-t*0.11)+32.83*exp(-t*12.01) Adj. R^2=0.99553

BTA-Man : BTA-OEG_4 1:1

y = 33.07*exp(-t*0.002)+37.21*exp(-t*21.63)+29.41*exp(-t*0.91) Adj. R^2=0.99823

y = 47.45*exp(-t*0.002)+30.78*exp(-t*0.93)+21.63*exp(-t*24.31) Adj. R^2=0.99854

BTA-OEG_4-Man : BTA-Man 1:1

y = 53.12*exp(-t*30.57)+27.24*exp(-t*0.002)+19.44*exp(-t*0.14) Adj. R^2=0.997

y = 31.57*exp(-t*0.003)+16.87*exp(-t*0.14)+51.46*exp(-t*42.34) Adj. R^2=0.99454

BTA-OEG_4-Man : BTA-OEG_4 1:1

y = 25.17*exp(-t*0.002)+25.87*exp(-t*1.83)+48.95*exp(-t*42.98) Adj. R^2=0.9997

y = 55.55*exp(-t*0.002)+21.36*exp(-t*1.60)+23.09*exp(-t*6.83E10) Adj. R^2=0.99816

4. Supplementary figures

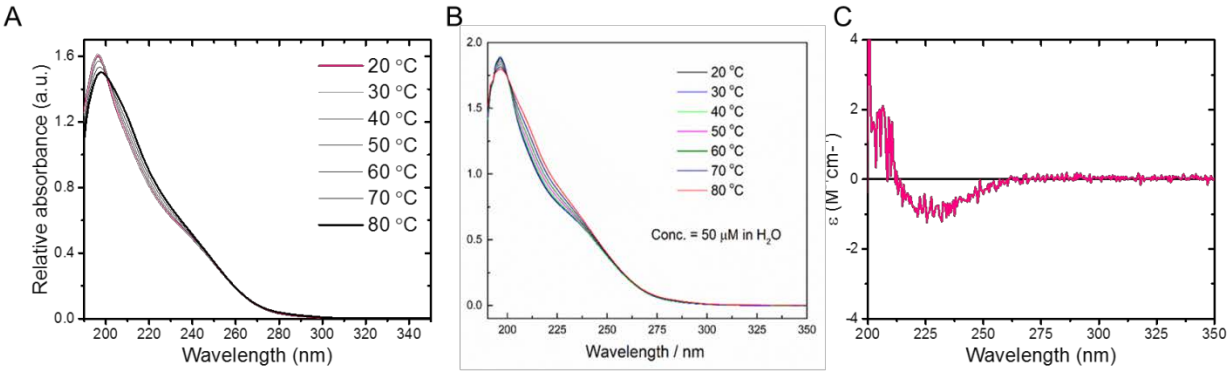

Figure S1: UV spectra of BTA-Cel (A) and BTA-OEG$_4$-Man (B) upon stepwise heating. CD spectrum of BTA-Cel (C). (c = 50 µM)

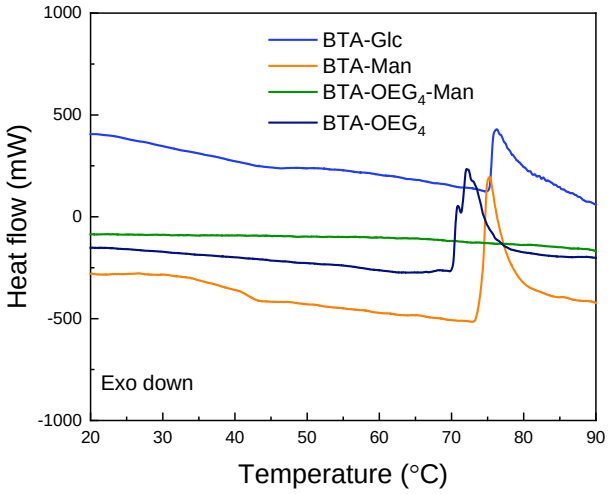

Figure S2: Micro-DSC heating curves of BTAs in MQ water with heating rate at 60 °C h^{-1}. (c = 500 µM).

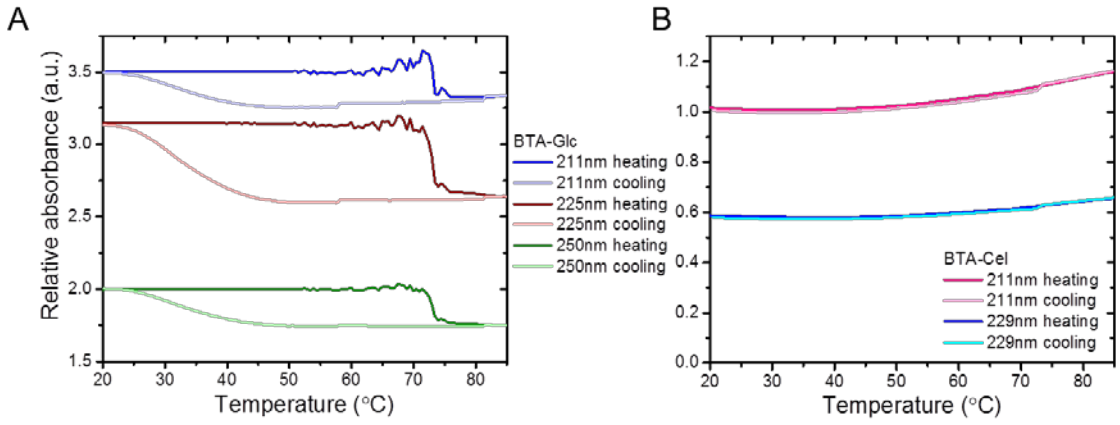

Figure S3: Continuous heating and cooling UV experiments of BTA-Glc (A) and BTA-Cel (B). (c = 50 µM).

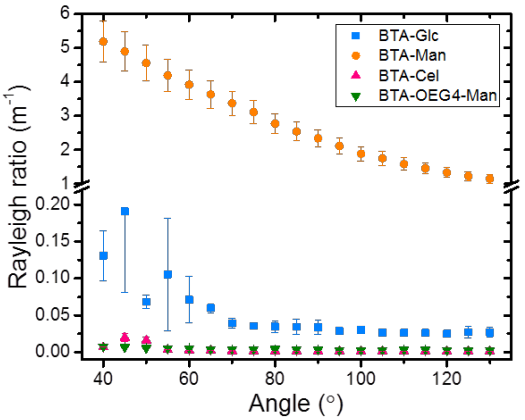

Figure S4: SLS of the homopolymers. (c = 500 µM).

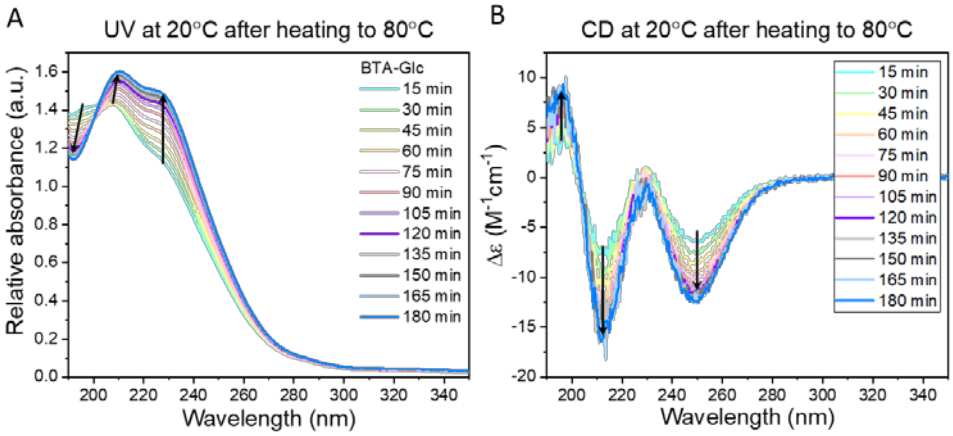

Figure S5: Investigating order recovery of BTA-Glc after heating. A) UV and B) CD spectra recorded every 15 minutes at 20°C after the sample was heated to 80°C and subsequently cooled to 20°C. ($c_{BTA\text{-}Glc}$=50µM)

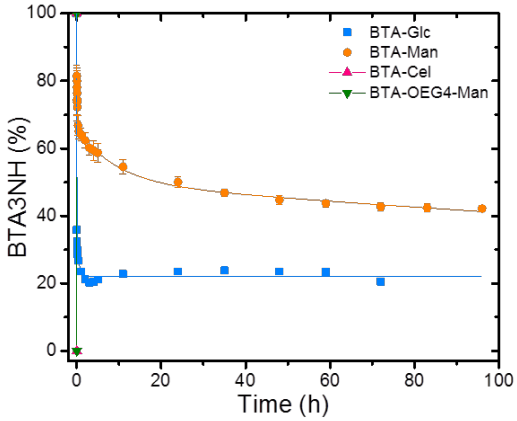

Figure S6: HDX-MS of the homopolymers. BTA-Man and BTA-Glc show a monomer exchange profile whereas BTA-Cel and BTA-OEG_4-Man are immediately fully deuterated upon dilution into D_2O. (Initial c = 500, c = 5 µM after dilution in D_2O).

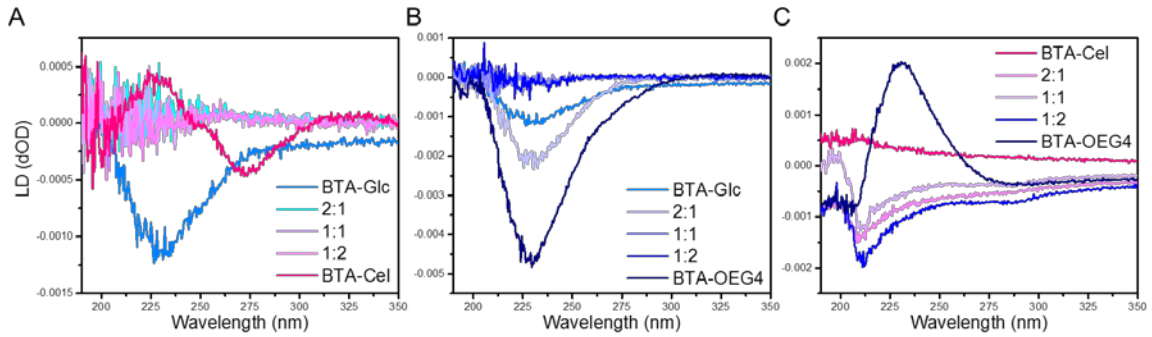

Figure S7: Linear Dichroism (LD) measurements of the copolymerization. BTA-OEG$_4$ displayed a strong LD effect, whereas the LD signal for the other samples was small only having a minimal effect on the CD. (c = 50 µM).

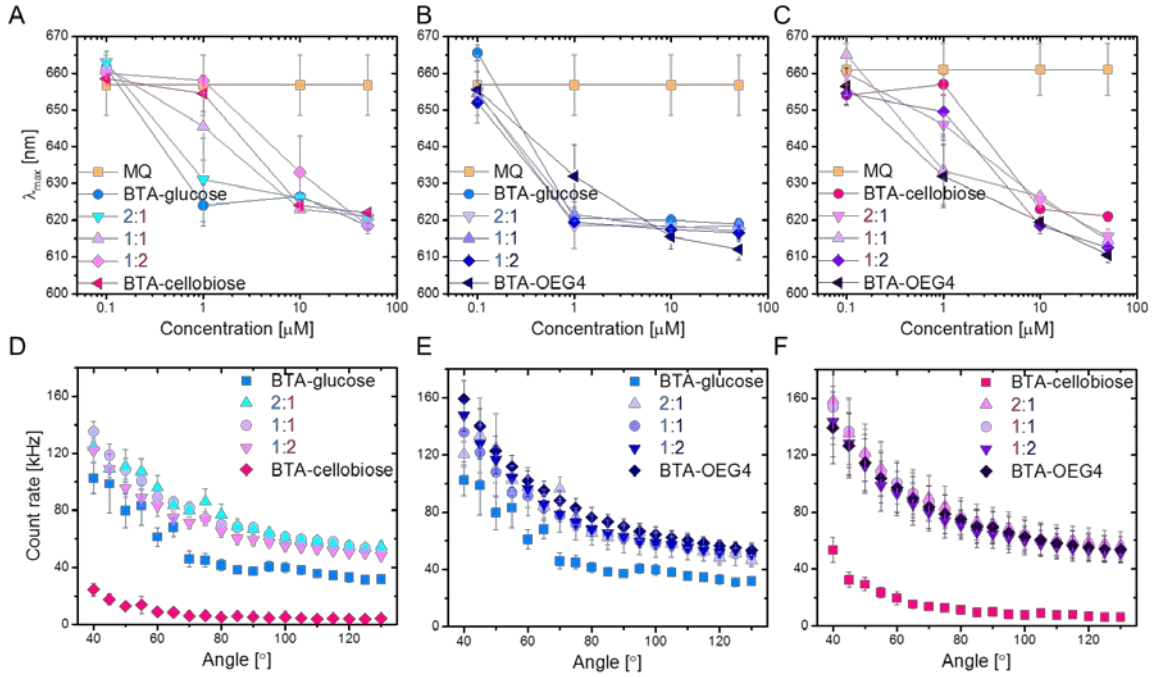

Figure S8: Nile red assay (top) and SLS measurements (bottom) of co-assembled BTAs in water at 20 °C. A) and D) BTA-Glc co-assembled with BTA-Cel. B) and E) BTA-Glc co-assembled with BTA-OEG$_4$. C) and F) Co-assembly of BTA-Cel with BTA-OEG$_4$. Nile red assay showed the existence of a hydrophobic pocket at micromolar concentrations. SLS revealed small aggregates for BTA-Cel, intermediate structures for BTA-Glc, and similar aggregate size for the mixtures as compared with BTA-OEG$_4$. A volume correction was applied to the SLS data. Error bars indicate standard deviation. ($c_{BTA,\ total}$ = 50, 10, 1, 0.1 µM for the nile red assays and $c_{BTA,\ total}$ = 250 µM)

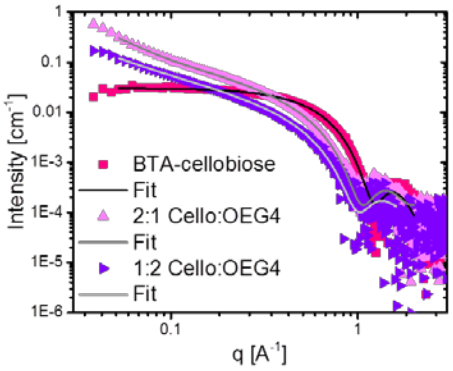

Figure S9: SAXS of BTA-Cel and its mixtures with BTA-OEG$_4$. BTA-Cel showed a plateau indicative of micellar structures, whereas for the co-assembled structures a slope was observed, suggesting fibrous assembly. ($c_{BTA,\ total}$ = 500 µM)

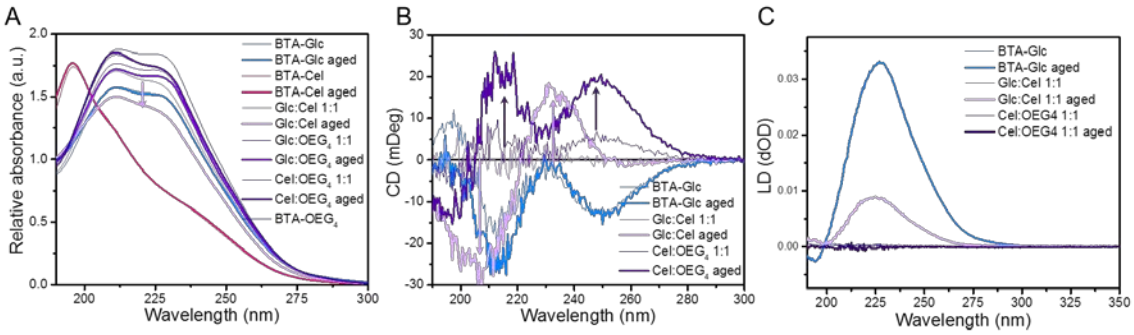

Figure S10: The influence of aging on the self-assembly. A) UV measurements taken of fresh samples and samples which were aged for 2 months, showing only a drop in absorbance for the Glc:Cel mixture. B) CD spectrum of the 3 samples with a difference in CD intensity. C) LD signal. BTA-Glc and Cel:OEG$_4$ both showed an enhanced CD effect over time, although for BTA-Glc it is a result of LD, whereas Glc:Cel showed an induction of helicity over time. ($c_{BTA,\ total}$ = 500 µM)

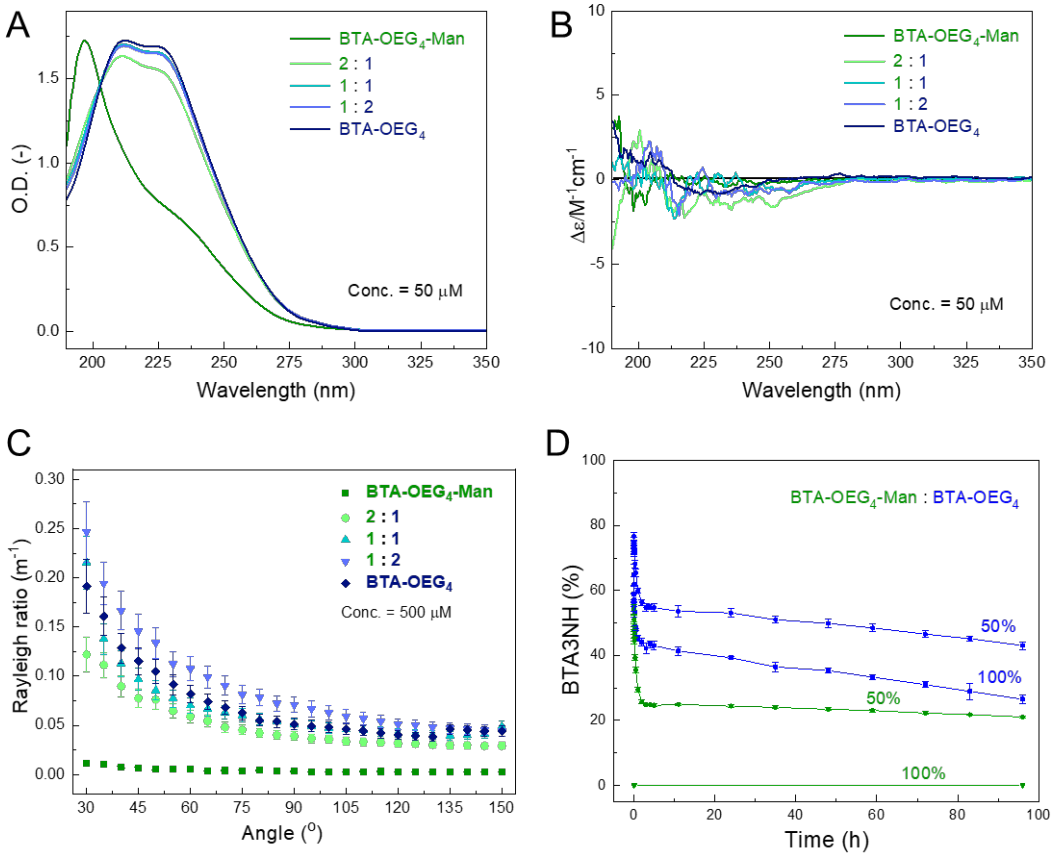

Figure S11: Supramolecular copolymerization of BTA-OEG4-Man and BTA-OEG4 with the ratios of 2:1, 1:1, and 1:2. A) UV spectra, B) CD spectra, and C) SLS measurements of two homopolymers and three copolymers, and D) HDX-MS of two homopolymer and the copolymer with 1:1 ratio.

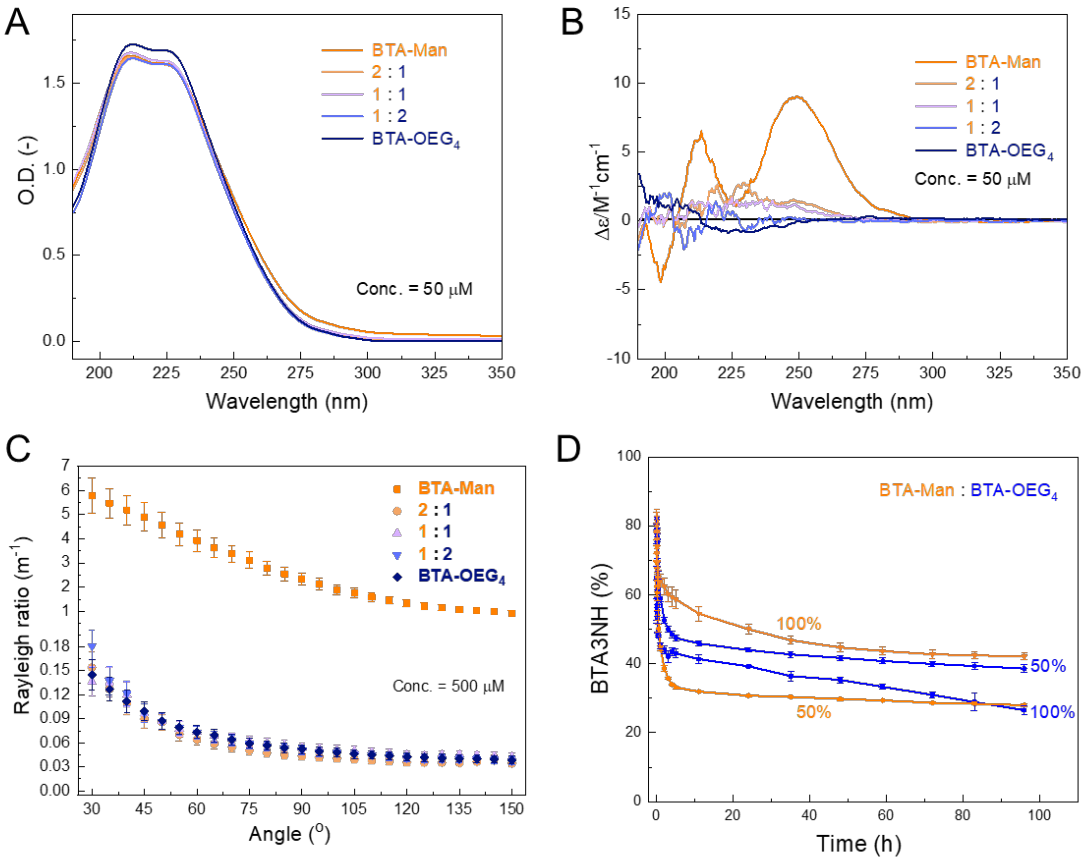

Figure S12: Supramolecular copolymerization of BTA-Man and BTA-OEG$_4$ with the ratios of 2:1, 1:1, and 1:2. A) UV spectra, B) CD spectra, and C) SLS measurements of two homopolymers and three copolymers, and D) HDX-MS of two homopolymer and the copolymer with 1:1 ratio.

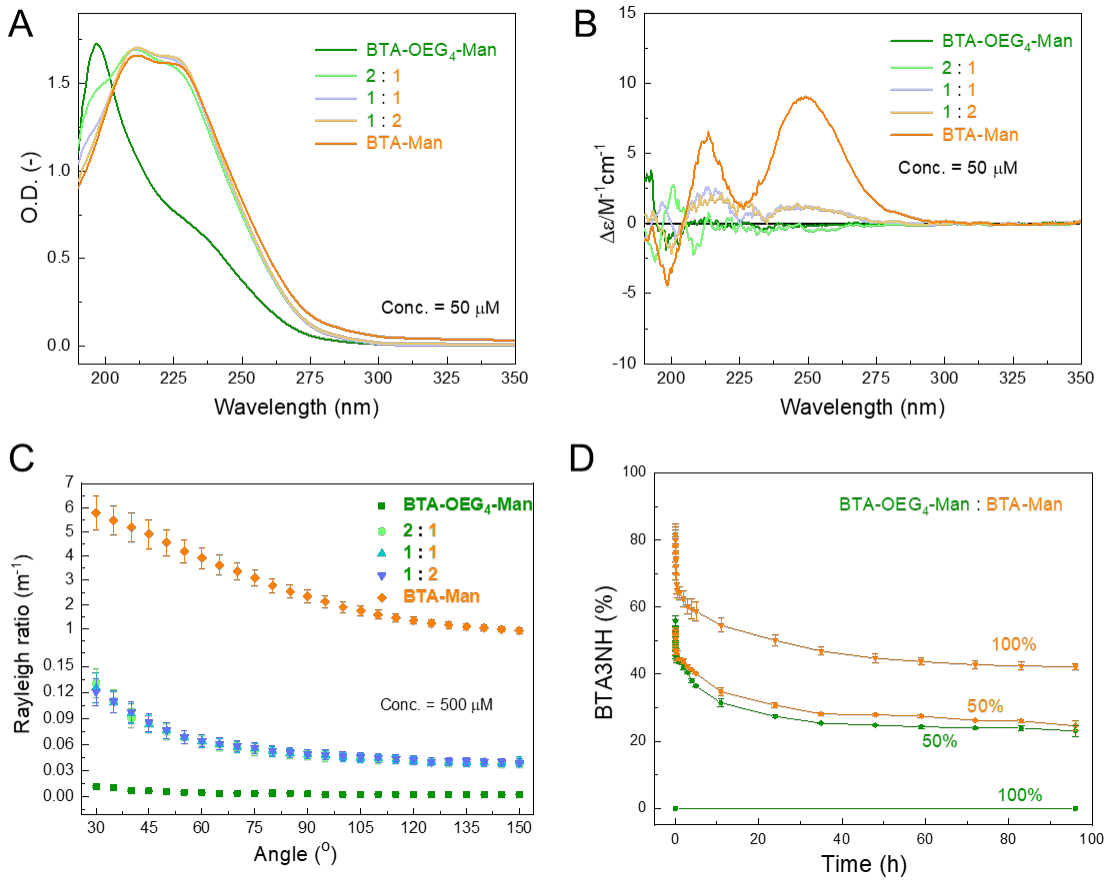

Figure S13: Supramolecular copolymerization of BTA-OEG$_4$-Man and BTA-Man with the ratios of 2:1, 1:1, and 1:2. A) UV spectra, B) CD spectra, and C) SLS measurements of two homopolymers and three copolymers, and D) HDX-MS of two homopolymers and the copolymer with 1:1 ratio.

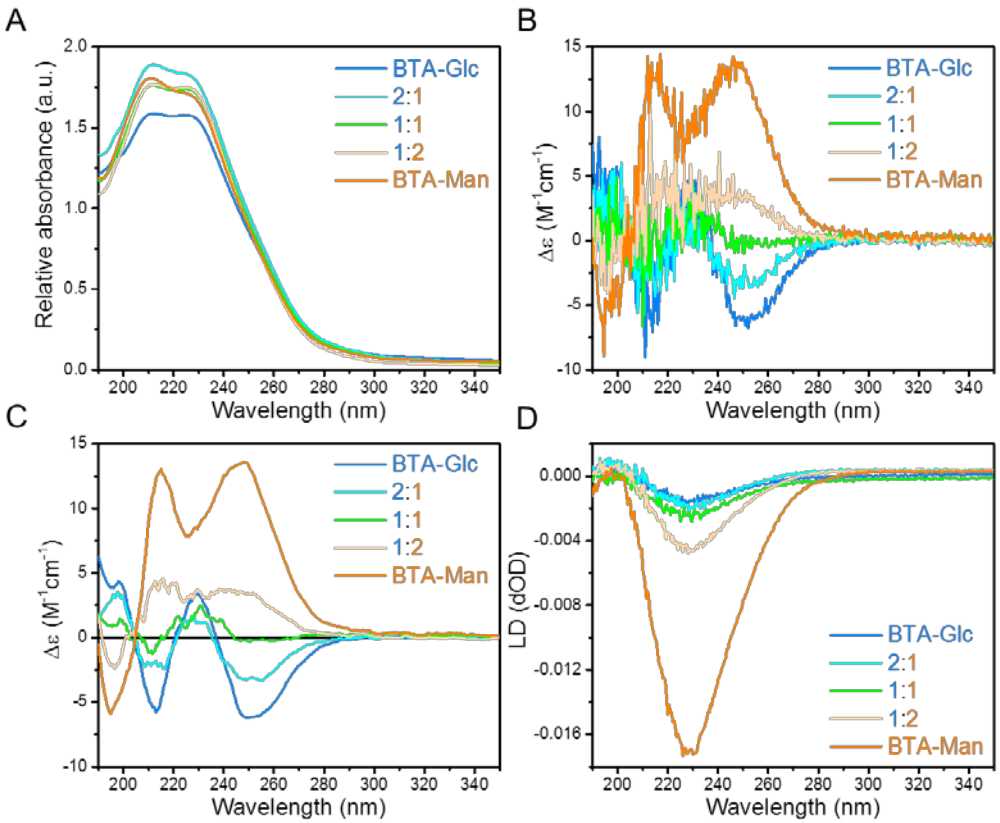

Figure S14: Supramolecular copolymerization of BTA-Glc and BTA-Man with the ratios of 2:1, 1:1, and 1:2. A) UV spectrum, B) CD spectrum, and C) smoothed CD spectrum to make the differences clearer and D) LD spectrum.

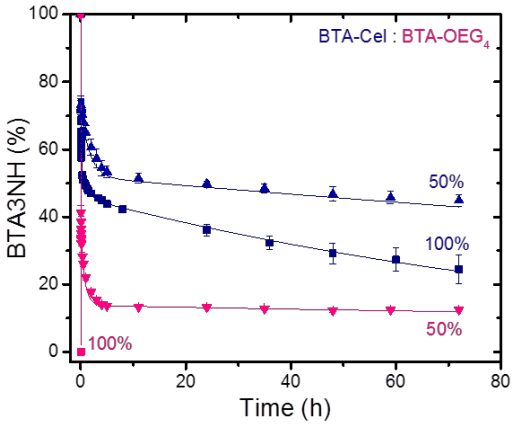

Figure S15: HDX-MS of the copolymer BTA-Cel: BTA-OEG_4 (1:1), as well as their homopolymers.

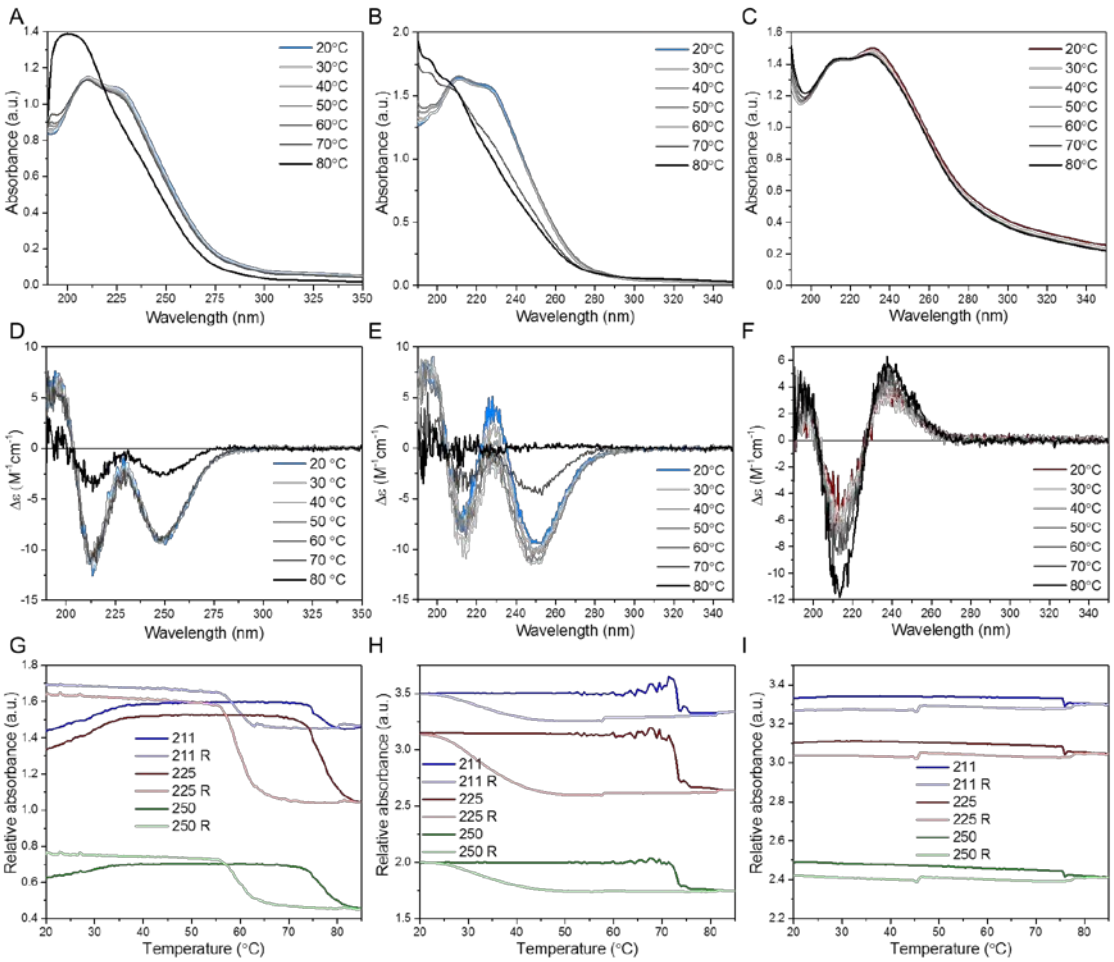

Figure S16: The influence of purity on BTA-Glc self-assembly. Left: measurements of BTA-Glc with >85% purity (15% 2-armed BTA), middle: BTA-Glc with >99% purity, and right: 2-armed BTA-Glc. A-C) UV measurements indicating a difference in aggregation behavior and stability upon heating the samples stepwise. D-F) CD measurements also indicating a difference in helicity upon different sample impurity. G-I) continuous heating and cooling ramp UV measurements showing a difference in disassemble and assemble temperature. ($c_{BTA,\ total}$ = 50 µM)

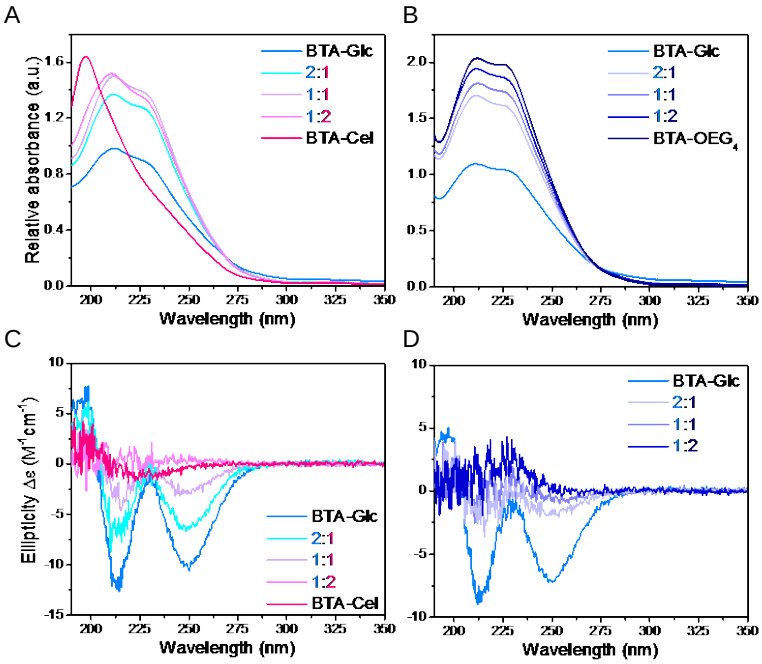

Figure S17: The influence of BTA-Glc composition on the co-assembly. BTA-Glc with >85% purity, including 15% 2-armed BTA was used as BTA-Glc. Top (A,B) UV spectra and bottom (C,D) corresponding CD spectra. BTA-Glc composition influences co-assembly as well. ($c_{BTA,\ total}$ = 50 µM).

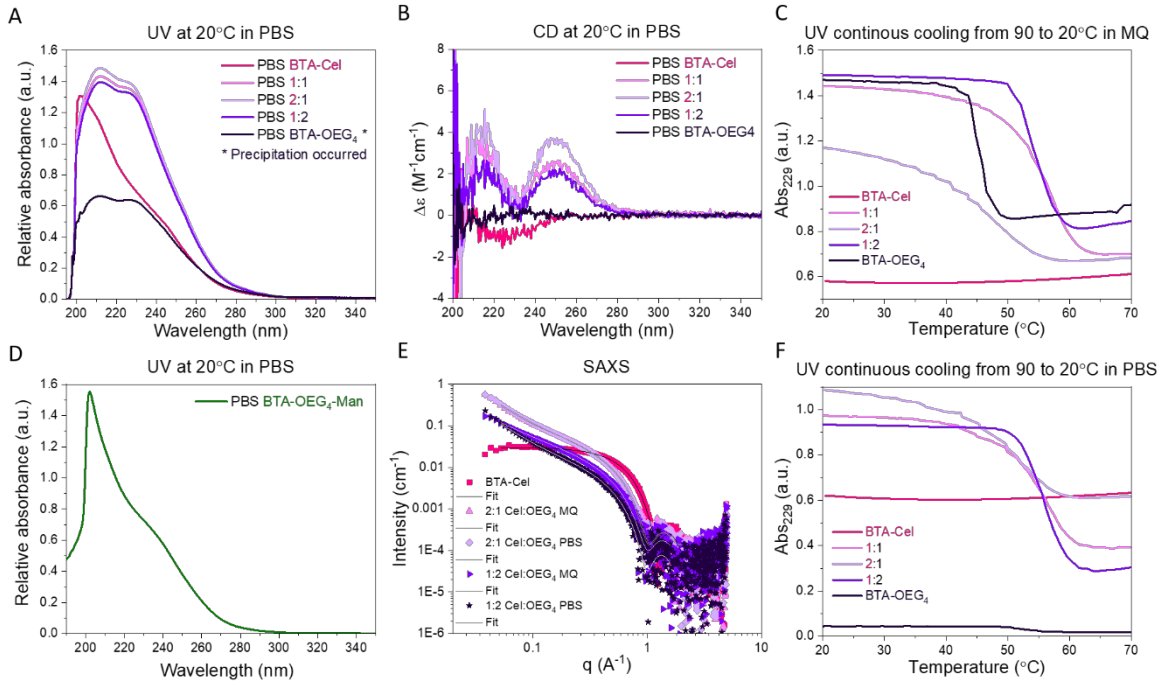

Figure S18: The influence of buffer on the self-assembly. A) UV of BTA-Cel and its corresponding co-assemblies with BTA-OEG$_4$ in PBS. B) The corresponding CD profiles. C and F) Continuous cooling experiment in which 90°C samples were slowly cooled to 20°C at a rate of 0.1°C/min. E) Corresponding SAXS measurements. D) UV of BTA-OEG$_4$-Man in PBS. BTA-Cel and BTA-OEG$_4$-Man did not self-assemble into elongated aggregates in buffer.

Copolymers showed similar SAXS profile as their counterparts in water. (c=50 μM or 250 μM for SAXS)

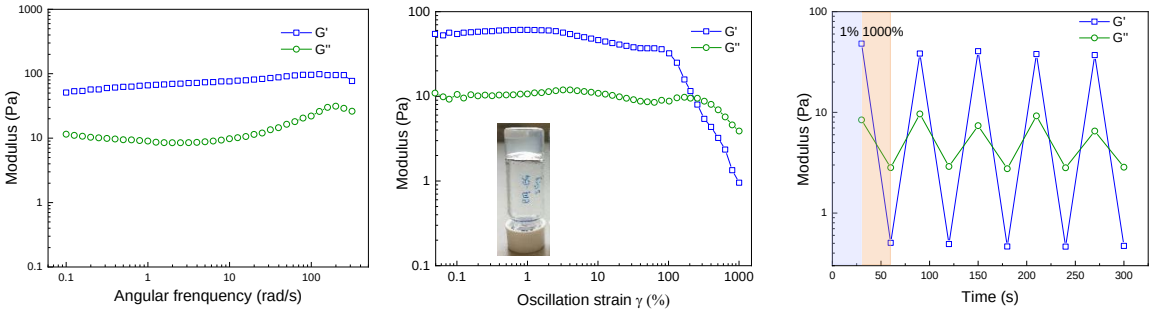

Figure S19: Left: Variation in storage and loss moduli (G', G'') with angular frequency at 37 °C (with a fixed applied strain of 1 %) for the 5 wt% hydrogel formed by BTA-OEG$_4$. Middle: Variation in storage and loss moduli with applied strain at 37 °C (with a fixed angular frequency of 1 rad/s) for the 5 wt% hydrogels. Inert: Photograph of inverted vial containing corresponding hydrogel. Right: Step-stain measurement with applied oscillatory stain alternated between 1 and 1000% for 30 s periods (with a fixed angular frequency of 1 rad/s, 37 °C) for the 5 wt% hydrogels. The process was repeated five times, showing good recyclability.

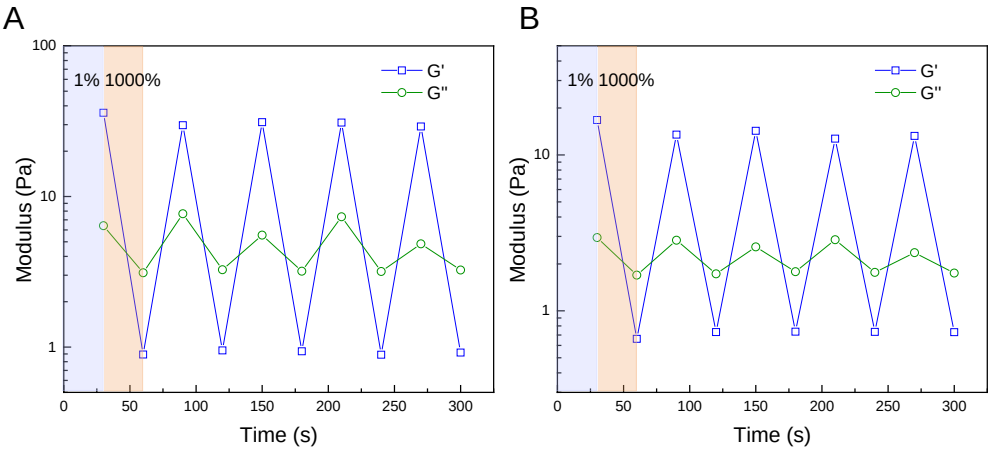

Figure S20: Step-strain measurements of **HG1** and **HG2** with applied oscillatory stain alternated between 1 and 1000% for 30 s periods (with a fixed angular frequency of 1 rad/s, 37 °C) for the 5 wt% hydrogels. The process was repeated five times, showing good recyclability.

5. References

(1) Wu, X.; Su, L.; Chen, G.; Jiang, M. Deprotection-Induced Micellization of Glycopolymers: Control of Kinetics and Morphologies. *Macromolecules* **2015**, *48* (11), 3705–3712.

(2) Leenders, C. M. A.; Albertazzi, L.; Mes, T.; Koenigs, M. M. E.; Palmans, A. R. A.; Meijer, E. W. Supramolecular Polymerization in Water Harnessing Both Hydrophobic Effects and Hydrogen Bond Formation. *Chem. Commun.* **2013**, *49* (19), 1963.

(3) Mbadugha, B. N. A.; Menger, F. M. Sugar/Steroid/Sugar Conjugates: Sensitivity of Lipid Binding to Sugar Structure. *Org. Lett.* **2003**, *5* (22), 4041–4044.

(4) Cammarata, A.; Upadhyay, S. K.; Jursic, B. S.; Neumann, D. M. Antifungal Activity of 2α,3β-Functionalized Steroids Stereoselectively Increases with the Addition of Oligosaccharides. *Bioorganic Med. Chem. Lett.* **2011**, *21* (24), 7379–7386.